

# The Phase Transition between Caged Black Holes and Black Strings – A Review

---

**Barak Kol**

*Racah Institute of Physics  
Hebrew University  
Jerusalem 91904, Israel  
barak\_kol@phys.huji.ac.il*

**ABSTRACT:** We now have two examples for the breakdown of black hole uniqueness in higher dimensional General Relativity: the black-hole black-string transition and the rotating black ring. In the last few years the phase diagram of the former was the subject of considerable study. The most surprising results seem to be the appearance of critical dimensions where the qualitative behavior of the system changes, and a novel kind of topology change. Recently, a full phase diagram was determined numerically, confirming earlier predictions for a merger point and giving very strong evidence that the end-state of the Gregory-Laflamme instability is a black hole (in low enough dimensions). Here this progress is reviewed, illustrated with figures, put into a wider context, and the still open questions are listed.

---

## Contents

<b>1. Introduction</b>	<b>2</b>
<b>2. Set-up and formulation of questions</b>	<b>5</b>
2.1 Background	5
2.2 Phases	6
2.3 Gregory-Laflamme instability	8
2.4 Issues	11
<b>3. Qualitative features</b>	<b>12</b>
3.1 Order parameter	12
3.2 Order of phase transition	14
3.3 Morse theory	18
3.4 Merger point	20
3.5 Phase diagrams – predictions and data	24
<b>4. Obtaining solutions</b>	<b>26</b>
4.1 2d gravito-statics	26
4.2 Numerical issues	32
4.3 Time evolution	34
4.4 Analytic perturbation method	37
<b>5. Related work</b>	<b>41</b>
<b>6. Summary and Open questions</b>	<b>42</b>
6.1 Results	43
6.2 Open questions	44
<b>A. Formulae for action manipulation</b>	<b>46</b>
<b>B. Topology change is a finite distance away</b>	<b>46</b>

---

To my girls,<sup>1</sup>  
Dorit, Inbal and Neta

## 1. Introduction

**Why study GR in higher dimensions?** There are several good reasons to study General Relativity (GR) in higher dimensions, namely  $D > 4$ , where  $D$  is the total space-time dimension. From a theoretical point of view there is nothing in GR that restricts us to  $D = 4$ . On the contrary, the theory is independent of  $D$ , and  $D$  *should be considered as a parameter*. It is common practice in theoretical physics to explore large regions of parameter space of a theory in order to enhance its understanding, rather than restrict to the experimental values and GR should be no exception. For example, in the study of gauge theories it is standard to consider various possibilities for the gauge group and matter content which differ from the standard model.

Additional reasons to study higher dimensional GR include *string theory* and the phenomenological scenario of “*large extra dimensions*”. String theory has a “built-in” preference for higher dimensional spacetimes with 10 (the “critical dimension”) or 11 dimensions, where the extra dimensions must be compactified. From the “large extra dimensions” scenario (which is string theory inspired) we wish to stress only the following important realizations: that to date gravity is measured only down to  $1\mu\text{-}1\text{mm}$  range (which is an “astronomically” poor resolution relative to the one we have for other forces), that it is quite consistent to assume the existence of a compact dimension(s) smaller than the experimental bound and that the situation can be rectified only by improving gravitational and accelerator experiments.

**The novel feature - non-uniqueness of black objects.** Often when we generalize a problem to allow for an arbitrary dimension the qualitative features do not change and thus the generalization does not produce “new physics”, even if the quantitative expressions are different. However, in GR we do find a qualitative change. If we roughly divide the field of General Relativity into black holes, gravitational waves and cosmology, we find a qualitative change in the first of these categories: one of the basic properties of 4d black holes changes, namely *black hole uniqueness*.

Here we should digress to make the distinction between two closely related black hole notions: “no hair” and “uniqueness”. “*No hair*” denotes the feature that the space of black hole solutions has a small dimension usually parametrized by asymptotically measured quantities (mass, angular momentum and electric charge, for example) much like macroscopic thermodynamical variables, while a non-black-hole star may have a much larger number of characteristics such as its internal matter ingredients each with its own equation of state and spatial distribution possibly resulting in an unbounded number of independent multipoles for mass, charge and angular momentum. This “no hair” spirit continues to hold in higher dimensional black holes as far as we know, in the sense that the number of parameters is small. Note however, that until recently all of these parameters

---

<sup>1</sup>wife and daughters

were conserved quantities, but now a family of black objects was found, namely the generalized rotating black ring [1, 2, 3], whose parameters include some non-conserved dipole charges.

“*Uniqueness*” on the other hand is the more specialized statement that a choice of all of these asymptotic black hole parameters selects a unique black hole rather than a discrete set. In 4d uniqueness was proven to hold, namely that given the mass, charge and angular momentum (satisfying some inequalities to ensure the existence of a solution with no naked singularities) there is a unique black hole. However, the proof relies heavily of properties which are special to 4d: Hawking’s proof that the horizon topology has to be  $S^2$ , and the simplifying gauge choices of Weyl-Papapetrou and Ernst (see [4] for references to original papers and reviews and for a speculative generalization of uniqueness to higher dimensions).

Here we pause to comment that the only other place in GR where I am aware of a qualitative dimensional dependence is in the Belinskii-Khalatnikov-Lifshitz (BKL) analysis of the approach to a space-like singularity, where there is a critical dimension  $D_{BKL}^* = 10$ , such that for  $D > D_{BKL}^*$  the system becomes non-chaotic (see the review [5] and references therein).

The breakdown of black hole uniqueness in higher dimensions implies the coexistence of several phases with the same asymptotic charges on a non-trivial phase diagram. *Phase transitions* between the various phases should occur as parameters are changed. As always one may define the order of the phase transition. It could be a first order transition in which case it is triggered non-perturbatively by a competition of entropies between two phases which are separated by a finite distance in configuration space, or it could be of second or higher order, in which case it is triggered by perturbative tachyons and the transition is smooth (see subsection 3.2).

Such first order transitions would be accompanied by an exceptional release of energy, sometimes called a *thunderbolt*, simply since the total mass of the final state must be lower or equal to that of initial state, and equality is highly unlikely as spacetime undergoes violent changes including sometimes the roll-down of a tachyonic mode resulting in energy loss through radiation.

**The two systems.** To date we know of two systems with higher dimensional non-uniqueness resulting in non-trivial phase transition physics

- The rotating ring
- The black-hole black-string transition

The first case is the rotating black ring in the flat (and topologically trivial) 5d background. Spherical rotating black holes solutions in higher dimensions, which generalize the 4d Kerr solution were already found in 1986 by Myers and Perry [6]. These solutions have an  $S^3$  horizon topology in 5d and display a maximal angular momentum (at fixed mass). In 2001 Emparan and Reall [7] discovered a beautiful solution, the ring, with horizon topology  $S^2 \times S^1$ , and with an angular momentum which is bounded from below, but not from

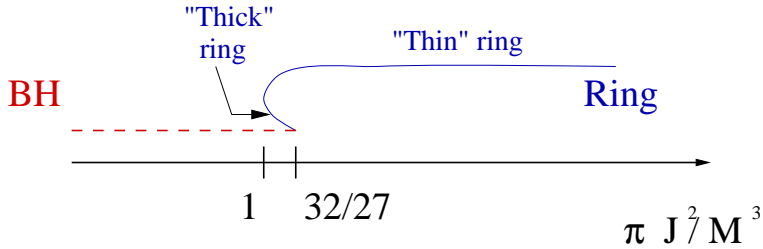


**Figure 1:** In asymptotically flat 5d spacetime uniqueness is violated by the co-existence of the rotating black hole and the rotating black ring. The figure shows the range of existence of each phase on the dimensionless angular momentum axis. Note that for  $1 \leq \pi J^2/M^3 \leq 32/27$  three phases co-exist.

above (at fixed mass). Figure 1 shows the regions on the angular momentum axis which are occupied by the various phases, and one notes that there is a middle region where three phases coexist – one black hole and two rings.

For some time it was not clear whether the black ring is stable. While many believed it to be unstable and hence unphysical (due to its unbounded size), the author of this review had the opposite hope, for otherwise “why does this solution exist?”. Very recently charged rings were shown to be BPS [8] and hence “super-stable” (that is, non-perturbatively stable). Several groups made progress in further generalizing these BPS solutions [9, 2, 3, 10], all of them restricted to 5d. The original non-BPS ring of [7] is not yet included in these new families, which are all BPS, but there is comfort in knowing that some of its closest relatives which share many of their outstanding properties are stable. Moreover, the inclusion of non-conserved dipole moments in [3] demonstrates the “no-hair” principle in higher dimensions must be generalized at least to allow for non-conserved quantities.

As the recent discovery of families of black rings demonstrates, we are far from knowing the full parameter space for rings, and we know close to nothing about the associated phase transitions.

At this point we set aside the topic of black rings until the discussion section and we turn in the next section to the other example for non-uniqueness, the black-hole black-string transition which is the main topic of this review. In section 2 the physical set-up is described and the questions of interest are formulated. In section 3 we describe the analytic considerations that culminate in subsection 3.5 to a certain qualitative form of the phase diagram which is compared there with numerical data. Section 4 describes the quantitative tools that were employed in order to obtain solutions, including both numerical and analytic methods. Finally, related work is described in section 5 and we conclude with a summary of the results and a discussion of open questions in section 6.

## 2. Set-up and formulation of questions

### 2.1 Background

We consider a background with extra compact dimensions. In such a background one expects to find several phases of black objects depending on the relative size of the object and the relevant length scales in the compact dimensions. For simplicity we discuss here pure GR (the only field is the metric) with no cosmological constant. Thus the backgrounds considered are of the form  $\mathbb{R}^{d-1,1} \times X^c$  where  $X^c$  is any  $c$ -dimensional compact Ricci-flat manifold,  $d$  is the number of extended spacetime dimensions, and the total spacetime dimension is  $D = d + c$ .

The simplest compactifying manifold is a single compact dimension  $X = \mathbf{S}^1$ , and that was the choice for most of the research so far, both for simplicity and since for more involved  $X$  it was expected to represent the essential phase transition physics between any two specific phases (generically). We denote the coordinate along the circle by  $z$  and we denote by  $L$  its size (or period), namely  $z \sim z + L$ . Sometimes we shall also refer to  $L$  for general  $X$  and then we loosely mean some characteristic size of  $X$ . Recently some research was devoted to  $X = \mathbf{T}^c$ , the  $c$ -dimensional torus [11], and we shall discuss it later. Other possibilities for  $X$  could be K3 and Calabi-Yau threefolds, as well as Ricci-flat  $X$  which are not supersymmetric.

Thus we consider a background with a single compact dimension of size  $L$ , namely  $\mathbb{R}^{d-1,1} \times \mathbf{S}^1$ , and  $D = d + 1 \geq 5$  (in order to avoid spacetimes with 2 or less extended spatial dimensions where the presence of a massive source is inconsistent with asymptotic flatness, see [12, 13, 14] for a limited analogue in  $D = 4$ ).

The non-rotating black objects in which we are interested are static and spherically symmetric. Thus, the essential geometry is 2d after suppressing time and the angular coordinates in the extended dimensions. Our coordinates are defined in figure 2.

This background is characterized by 3 dimensionful parameters  $M$ ,  $L$  and  $G_N$  where  $M$  is the mass of the black object (measured in the asymptotic  $d$  dimensional spacetime, and the detailed expression is given in eq. 3.5), and  $G_N$  is Newton's constant. These define a single dimensionless parameter <sup>2</sup>

$$\mu := \frac{G_N M}{L^{D-3}} . \quad (2.1)$$

Alternatively one may use a different parametrization of the solutions such as replacing  $M$  by  $\beta$ , the inverse temperature.<sup>3</sup> Correspondingly one may define another dimensionless parameter

$$\mu_\beta \propto \frac{\beta}{L} , \quad (2.2)$$

where the proportionality factor may be chosen later by convenience. Sometimes when we want to distinguish the dimensionless parameters above we may denote  $\mu$  by  $\mu_M$  to stress its dependence on the mass.

---

<sup>2</sup>We are dealing with classical GR, and thus we *do not* set  $\hbar = 1$ .

<sup>3</sup>More precisely in order to avoid using  $\hbar$  we define here  $\beta = 2\pi/\kappa$ , namely the period of the Euclidean time direction, and  $\kappa$  is the surface gravity.

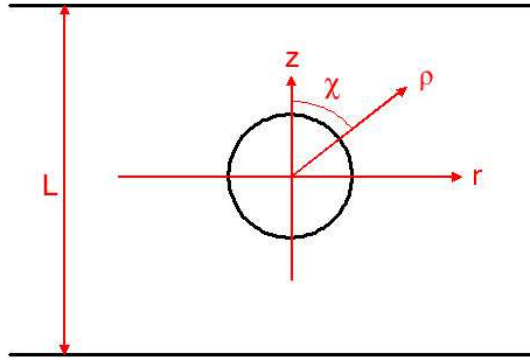


**Figure 2:** Definition of coordinates. For backgrounds with a single compact dimension the essential geometry is 2d after suppressing time and angular coordinates in the extended dimensions. The cylindrical coordinates  $(r, z)$  are defined such that  $z \sim z + L$  is the coordinate along the compact dimension and  $r$  is the radial coordinate in the extended spatial directions. For black holes we define another set of local coordinates  $(\rho, \chi)$ , defined only for  $\rho \leq L/2$ , which are radial coordinates in the 2d plane with origin at the center of the BH.

In this background one expects at least two phases of black object solutions: when  $\mu \ll 1$ , namely the size of the black object is small (compared to  $L$  the size of the extra dimension) one expects the region near the object to closely resemble a  $D$ -dimensional black hole, while as one increases the mass one expects that at some point the black hole will no longer fit in the compact dimension and a black string, whose horizon winds around the compact dimension will be formed.

Definition: We distinguish between the *black hole* (BH) and the *black string* according to their *horizon topology* which is either spherical —  $S^{D-2}$  or cylindrical —  $S^{d-2} \times X$ , respectively.

We shall sometimes refer to such a black hole localized in a compact dimension as a “*caged black hole*”. See figures 3,4,5(b).

**Applications .** In addition to the intrinsic value of this system it has attracted continued interest in String Theory, particularly regarding the higher dimensional origin of brane solitons (such as the M-theory origin of string branes), where the physics is significantly affected by the question whether they are localized in the compact dimensions or wrap them.

## 2.2 Phases

**The black string.** We can readily write down solutions which describe *uniform black strings* (see figure 3)

$$ds^2 = ds_{\text{Schw}}^2 + ds_X^2 \quad (2.3)$$

where  $ds_X^2$  is the metric on  $X$ , which for our central example, an  $S^1$  parametrized by the coordinate  $z$ , is just

$$ds_X^2 = dz^2, \quad (2.4)$$

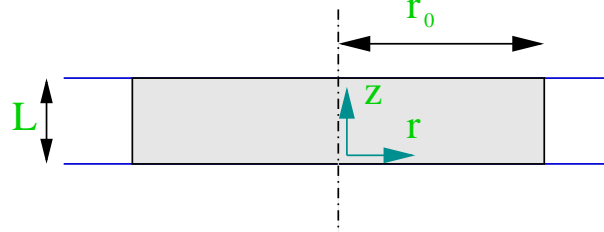


**Figure 3:** The uniform black string.  $r_0$  is its Schwarzschild radius.

and  $ds_{\text{Schw}}^2$  is the  $d$ -dimensional Schwarzschild black hole (also known as Schwarzschild-Tangherlini [15]), which is given by

$$ds_{\text{Schw}}^2 = -f(\rho) dt^2 + \frac{1}{f(\rho)} d\rho^2 + \rho^2 d\Omega_{d-2}^2 \quad (2.5)$$

where

$$f(\rho) = 1 - \frac{\rho_0^{d-3}}{\rho^{d-3}}, \quad (2.6)$$

$d\Omega_{d-2}^2$  is the metric on the sphere  $S^{d-2}$

$$d\Omega_{d-2}^2 = d\chi^2 + \sin^2 \chi d\theta_1^2 + \dots + (\sin^2 \chi \sin^2 \theta_1 \dots \sin^2 \theta_{d-4}) d\theta_{d-3}^2. \quad (2.7)$$

$\rho_0$  is related to the black hole mass,  $M$ , via [6]

$$\rho_0^{d-3} = \frac{16 \pi G_d M}{(d-2) \Omega_{d-2}}, \quad (2.8)$$

where  $G_d$  is the  $d$ -dimensional Newton constant, and  $\Omega_{d-1} = d \frac{\pi^{d/2}}{(d/2)!} = \frac{2\pi^{\frac{d}{2}}}{\Gamma(\frac{d}{2})}$  is the area of a unit sphere  $S^{d-1}$ . The relation between  $r_0$  and the inverse temperature  $\beta$  is

$$\beta = \frac{2\pi}{\kappa} = \frac{4\pi}{f'(r_0)} = \frac{4\pi r_0}{d-3}. \quad (2.9)$$

These metrics are Ricci flat as a result of being a direct product of Ricci flat metrics. They are called “uniform” for being a direct product with  $X$  (moreover, for  $\mathbf{S}^1$  the full metric is independent of  $z$ ). Later we will encounter also *non-uniform strings* (see figure 5(b)). Note that for general  $c$  (namely  $\dim(X)$ ) it would be more appropriate to call these metrics “black  $c$ -branes” rather than strings.

The uniform black string solution is valid for any  $r_0$  (and fixed  $X$ ). However, we shall soon see that for “thin” strings, namely small enough  $r_0$ , an instability develops.

**Caged black holes.** One expects localized black hole (BH) solutions to exist (see figure 4), intuitively obtained by constructing a black hole locally without ever being “aware” of the compactness of some of the dimensions, at least as long as the black hole is much smaller than the compact dimensions (and the number of extended spacetime dimension is  $d \geq 4$  to avoid problems with asymptotics).

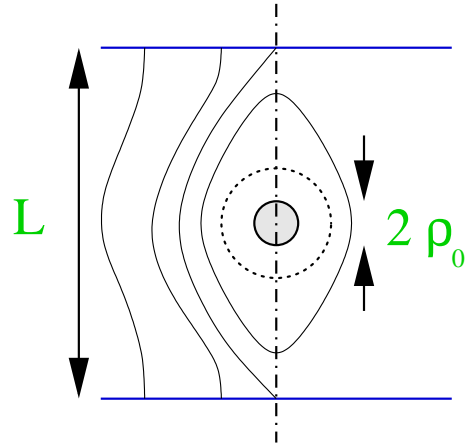


**Figure 4:** A caged black hole (BH). Newtonian equipotential lines are shown.

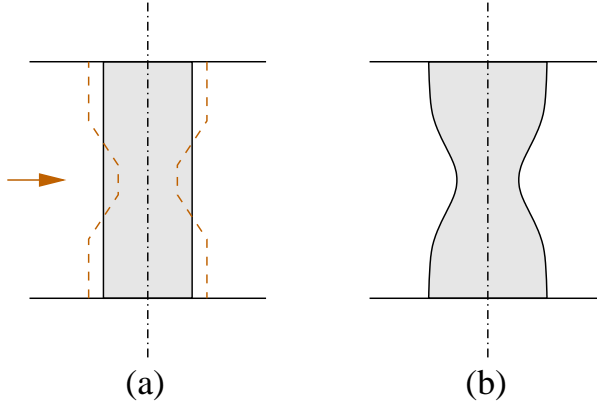


**Figure 5:** (a) The Gregory-Laflamme instability. (b) A non-uniform black string.

As the black hole grows it will start feeling the presence of the compact dimensions and it will deform accordingly. As some critical  $\mu$  one may expect that the black hole will be too large to fit into  $X$ , and so the mass of this phase will be bounded from above.

Unlike the uniform black string there is no explicit analytical metric that we can write down. This situation was confronted by two methods: an analytical perturbative expansion [16, 17, 18] and numerical simulations [19, 20, 21, 22]. Both techniques will be described in section 4, and here we only note that the analytic method is useful for small black holes (actually  $\mu_\beta$  is the small parameter for the perturbation series), while for large black holes, where the interesting phase transition physics occurs the numerical methods are essential. The existence of both techniques created a healthy feedback where both methods were used to test and improve each other.

### 2.3 Gregory-Laflamme instability

Gregory and Laflamme (GL, 1993 [23]) discovered that the uniform black string solution (2.5) develops a  $z$ -dependent tachyon below a certain critical mass [23] (see figure 5). By a “tachyon” one means that when one analyzes the spectrum of frequencies-squared for small

perturbations around this background, a negative eigenvalue is found.<sup>4</sup> The main results of GL are summarized in the figure 6 (taken from [23, 25]) which depicts the negative frequency-squared as a function of  $r_0/L$  for total spacetime dimensions  $5 \leq D \leq 10$ .

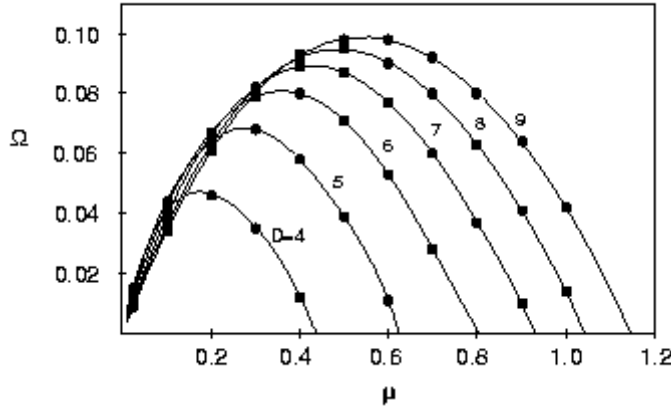


**Figure 6:** Characteristic decay times  $\Omega$  (giving the perturbation an  $e^{\Omega t}$  time dependence) as a function of the perturbation wavenumber  $\mu := \pi r_0/L = r_0 k/2$  (proportional to  $\mu_\beta$  in our notation) for  $4 \leq D \leq 9$  where  $D$  is the extended space-time dimension ( $d$  in our notation) in backgrounds with an  $\mathbf{S}^1$  compactification.  $k_{GL}$ , the critical Gregory-Laflamme wave-numbers, are the maximal wavenumbers for which the instability exists. Reproduced from [23, 25].

From figure 6 we see that the tachyonic mode appears for wavenumbers  $k$  (at fixed  $r_0$ ) which are lower than a critical wavenumber  $k_{GL}$  (which depends on  $d$ ). In order to find  $k_{GL}(d)$  it is not necessary to look at perturbation in  $D$  dimensions, but rather it suffices to find the negative mode of the Euclidean  $d$  dimensional Schwarzschild black hole. This mode, discovered by Gross, Perry and Yaffe [26] (in the 4d case) and hence denoted here by  $h_{GPY}$  satisfies

$$L_{Schw} h_{GPY} = -\lambda_{GPY} h_{GPY} \quad (2.10)$$

where  $L_{Schw}$  is the Lichnerowicz operator for perturbations in the Schwarzschild background and  $-\lambda_{GPY}$  is the negative eigenvalue. Given  $h_{GPY}$  the marginally tachyonic mode is given by

$$h = h_{GPY} \exp(i k_{GL} z) \quad k_{GL} := \sqrt{\lambda_{GPY}} \quad (2.11)$$

In [27] the critical GL lengths were obtained for Schwarzschild black holes in various dimensions (see table 1). From these the high  $d$  asymptotic form was extracted and later

<sup>4</sup>It is interesting to note that one of the original objectives of GL was to show that branes, a concept made popular by string theory, are unstable, and by showing that make a dent in string theory itself. Of course we now know that many of the fundamental branes of string theory are supersymmetric and hence automatically (non-perturbatively) stable. So as is often the case, an important discovery was made, partially based on incorrect motivations. Another curiosity is that the same collaboration first concluded in 1988 that the black strings were stable [24] and only later found the tachyon.

proven analytically in [11] to be

$$k_{GL} \simeq \sqrt{d} \frac{1}{r_0} . \quad (2.12)$$

This means that for large  $d$  the black string becomes unstable at a compactification length  $L_{GL} = 2\pi/k_{GL} \sim r_0/\sqrt{d}$  when it is quite “fat” (namely  $r_0 \gg L_{GL}$ ) and indicates that such a string would not decay into a black hole which would not “fit” inside the extra dimension.

At  $k = k_{GL}$  the GL mode is marginally tachyonic, namely a zero-mode. Morse theory arguments (see subsection 3.3) guarantee that this zero-mode produces a branch of solutions emanating from the GL point describing non-uniform strings due to the  $z$ -dependence of the GL mode.

d	4	5	6	7	8	9	10	11
$k_{GL}$	.876	1.27	1.58	1.85	2.09	2.30	2.50	2.69
d	12	13	14	15	19	29	49	99
$k_{GL}$	2.87	3.03	3.19	3.34	3.89	5.06	6.72	9.75

**Table 1:** Numerically computed static mode wavenumbers  $k_{GL}$  in units of  $r_0^{-1}$  as a function of  $d$ , the number of extended space-time dimensions [11].

**The end-state.** Whenever one discovers a perturbative tachyon indicating a decay, the question of its end-state is naturally raised. As the end-state configuration often lies away from the initial configuration a perturbative analysis does not suffice and one needs global information regarding all stable static solutions which is more difficult to obtain.

Gregory and Laflamme believed the end-state to the black hole, both since that was the only other phase they knew about and since comparing entropies at small  $\mu$  one notices that the black hole phase has superior entropy in this regime. Indeed for small  $\mu$ , where the black hole is well approximated by a  $D$  dimensional spherical black hole, the entropies scale as

$$S_{BH} \sim r_0^{D-2} \sim \mu^{\frac{D-2}{D-3}} \\ S_{St} \sim r_0^{d-2} \sim \mu^{\frac{d-2}{d-3}} , \quad (2.13)$$

in units where  $L = G_d = G_D = 1$ . It is seen that the exponent  $(D-2)/(D-3) = 1+1/(D-3)$  is a monotonically decreasing function of its argument and hence the exponent is smaller for  $D > d$  (the black hole) resulting in a larger area.

More recently Horowitz and Maeda [28] made the surprising claim that a black hole could not be the end-state of decay and predicted instead the existence of a stable non-uniform string phase that would serve as an end-state. The argument relied on assuming the increasing area theorem for an event horizon and applying it to an area element at the “waist” – the inward collapsing region of the event horizon. While this claim stimulated much of the research reported here, strong evidence against it will be described as this review proceeds, and it is the opinion of the author that the end-point is actually the black hole phase as originally argued by Gregory and Laflamme (at least in dimension  $D \leq 13$ ). See the summary section for a more complete discussion.

## 2.4 Issues

Let us formulate some major issues or questions regarding this phase transition. These issues may be roughly divided into two groups: static and time evolution.

The static issues include

- End-state of decay.
- Qualitative form of the phase diagram including the determination of all static phases.
- Detailed quantitative data on the phase diagram: the domain of existence of each phase and the determination of critical points.

During the last couple of years there was significant progress on the static issues, resulting also in the surprising discoveries of critical dimensions and a topology change. The deepest issues belong however to the time evolution

- The spacetime structure, namely determination of the Penrose diagram.
- A naked singularity and a violation of Cosmic Censorship.

It is plausible that as the black string pinches a naked singularity is formed, naively because the singularity which “originally” winds the compact dimension gets “broken”, perhaps at the event of pinching. Another argument comes from the clash between the arguments of [28] and results on the system’s phase diagram [29, 22]. Since the derivation of [28] is solid, it is quite clear that only deep issues could have gone wrong there, and I expect that the problem has to do with the assumption that there are no singularities strictly outside the horizon. Note that the initial conditions in this case are generic, unlike known examples of naked singularities.

- A thunderbolt and quantum gravity.

The decay is accompanied by a release of energy (after all, a tachyon is involved) in the form of radiation (see [30]). It is plausible that this radiation pulse is classically singular (a “thunderbolt”), perhaps due to its origin from the naked singularity. In such a case it is quite plausible that some knowledge of quantum gravity will be necessary in order to understand this outgoing radiation.

While there was much progress on the static issues, there was practically none on the time evolution issues, and these remain unsolved.

### 3. Qualitative features

In order to understand the phase transition physics and to resolve the issue of the end-state it suffices to map out all static and stable solutions of the system, since the end-state is certainly static and stable. But actually, Morse theory arguments will lead us to consider all static solutions whether stable or not, in order to take advantage of a “phase conservation rule” which is a powerful qualitative constraint on the form of the phase diagram. So we seek the phase diagram of all static solutions as a function of  $\mu$ , and throughout this review we will restrict ourselves to static aspects of the system.<sup>5</sup>

In this section we seek to determine the phase diagram qualitatively, and the quantitative aspects will be described in the next section.

#### 3.1 Order parameter

We wish to define an order parameter  $\lambda$  such that the uniform string will have  $\lambda = 0$  and the emerging non-uniform branch (from the GL point) will have  $\lambda \neq 0$ , namely  $\lambda$  should be a measure of non-uniformity. Actually, it is desirable to have both the black strings and the black holes at finite values of  $\lambda$ , motivated by Morse theory arguments that will be explained in subsection 3.3.

It turns out that an asymptotic analysis of the metric and the associated charges furnishes physically meaningful candidates [31, 19]. For concreteness, we take the compactification manifold to be  $X = \mathbf{S}^1$  throughout this subsection. Far away from the black object the leading behavior of the radial coordinate  $r$  is well-defined (by comparison with the flat geometry) and the metric becomes  $z$ -independent ( $z$ -dependent modes are massive from the lower dimensional point of view and hence they decay like  $\exp(-2\pi n r/L)$ ,  $n \in \mathbb{Z}$ ). Asymptotic  $z$ -independence means that it is sensible to perform a dimensional reduction. After dimensional reduction  $g_{zz}$ , the size of the extra dimension, turns into a scalar field. Thus we expect *two asymptotic charges – the mass and the scalar charge* (the latter is non-conserved, as usual).

One can define the asymptotic charges from either the higher dimensional or from the dimensionally reduced points of view. In the higher dimension the metric defines two asymptotic constants  $a, b$

$$\begin{aligned} -g_{tt} &= 1 - \frac{2a}{r^{d-3}} \\ g_{zz} &= 1 + \frac{2b}{r^{d-3}}. \end{aligned} \tag{3.1}$$

From the lower dimension point of view the definition for  $b$  conforms with the standard definition of a scalar charge. The dimensionally reduced metric is gotten by a Weyl rescaling of the metric  $g_{tt} \rightarrow \tilde{g}_{tt} = g_{zz}^{1/(D-3)} g_{tt}$  and therefore  $\tilde{a} = a - b/(D-3)$ , where  $\tilde{a}$  is defined by  $-\tilde{g}_{tt} = 1 - 2\tilde{a}/r^{d-3}$ . Identifying  $2\tilde{a}$  with  $r_0^{d-3}$  and using (2.8) we get

$$G_d M = \frac{\Omega_{D-3}}{8\pi} [(D-3)a - b]. \tag{3.2}$$

---

<sup>5</sup>Except for subsection 4.3 where a simulated time evolution is described.

	Uniform string	Small black hole
Scalar charge	0	$G_d M/(D-3)$
Tension	$M/(D-3)$	0

**Table 2:** Values for some possible order parameters for both “extreme” phases

The asymptotic constants  $a, b$  can be expressed in terms of *two physical charges, the mass  $M$  and the tension  $\tau$* . In a satisfying analogy with the well-known first law of gas thermodynamics

$$dE = T dS - P dV , \quad (3.3)$$

where  $E, T, S, P, V$  are the energy, temperature, entropy, pressure and volume, respectively,  $M$  and  $\tau$  are defined here through

$$dM = T dS + \tau dL . \quad (3.4)$$

Namely, the tension is defined to be the thermodynamic conjugate to  $L$ , the size of the extra dimension (see [32, 33] for earlier and equivalent definitions of tension).

The thermodynamic charges are related to the asymptotic constants  $a, b$  through

$$\begin{bmatrix} M \\ \tau L \end{bmatrix} = \frac{\Omega_{D-3}}{8\pi} \begin{bmatrix} D-3 & -1 \\ 1 & -(D-3) \end{bmatrix} \begin{bmatrix} a \\ b \end{bmatrix} . \quad (3.5)$$

This relation may be derived either through the thermodynamic definitions or from the “method of equivalent sources”. The thermodynamics is fully specified by the gravitational (Gibbons-Hawking) action  $I = -\beta F$  where  $\beta$  is the inverse temperature and  $F$  is the free energy. Alternatively, in the “method of equivalent sources” one imagines that the asymptotic fields were generated by a weak stress-energy source and uses the linearized equations to infer from these asymptotics the integrated stress-energy charges. Note that our thermodynamic definition for the mass yields an expression (3.5) which coincides with the mass read off the dimensionally reduced metric (3.2).

Let us gain some insight into the behavior of the tension and the scalar charge. For the uniform string  $b = 0$ , and hence  $\tau = M/(D-3)$ . For the small black hole one finds from the Newtonian approximation that  $\tau = 0$  and  $b = G_d M/(D-3)$ . More precisely, to leading order the tension is proportional to  $M^2$ :  $\tau L = (D-3) \zeta (D-3)/2 (\rho_0/L)^{D-3} M$  [16]. See table 2 for a summary.

Inverting (3.5) we obtain

$$\begin{bmatrix} a \\ b \end{bmatrix} = \frac{8\pi}{\Omega_{D-3}(D-4)(D-2)} \begin{bmatrix} D-3 & -1 \\ 1 & -(D-3) \end{bmatrix} \begin{bmatrix} M \\ \tau L \end{bmatrix} . \quad (3.6)$$

Looking at the expression for the scalar charge  $b$  we see that the mass tends to increase it, namely mass “wants to generate more space” for itself, while tension “wants” to contract the extra dimension. Thus we may say that for the uniform string ( $b = 0$ ) the tension has exactly the correct value to cancel the tendency of mass to expand the extra dimension.

In fact we empirically find that for all black hole and black string solutions their  $b, \tau$  parameters lie between the uniform string and the small BH. This is only partly understood. Positive tension  $\tau > 0$ , was proven in analogy with the positive mass theorem [34, 35]. However, it is not clear so far why  $b > 0$  holds. Actually, when one considers also bubbles (for instance [36]) then  $b$  is no longer positive. While  $b > 0$  would correspond to the bound  $\tau L/M < 1/(D-3)$  it was argued in [31] (see also [37]) that the completely general bound is higher, namely  $\tau L/M < (D-3)$ . This bound is set by the bubble and is consistent with the Strong Energy Condition  $T_{00} - 1/(D-2)T_\mu^\mu g_{00} > 0$ .<sup>6</sup>

Since  $b$  is zero exactly for the uniform string it can serve as a natural order parameter of non-uniformity. Moreover, we choose to use a dimensionless scalar charge as an order parameter. The dimensionless combinations are  $b/(G_d M)$  or  $b/\beta^{d-3}$  for the micro-canonical or canonical ensembles, respectively. Alternatively, one can use a dimensionless tension, such as  $\tau/M$ , as an order parameter. From our discussion above we see that indeed all phases lie at finite values of the order parameter. Another property of the phase diagram is that intersections in the phase diagram are constrained [31].

Here we wish to note that the differential form of the first law of black hole thermodynamics (3.4) may be integrated using the scale invariance of GR and yields

$$(D-3)M = (D-2)T S + \tau L , \quad (3.7)$$

which is a useful formula known as “*the integrated first law*” or “Smarr’s formula” (shown in this context in [31, 19]).

### 3.2 Order of phase transition

In general one of the basic properties of any phase transition is its order. In this subsection we first review the general Landau-Ginzburg theory and then we summarize the results for the system under study.

In a phase transition some derivative of the free energy is discontinuous and goes through a jump. The order of a phase transition is defined to be the order of this derivative. A first order transition is between two phases which are separated in configuration space and hence have different entropies (and other thermodynamic variables) while for second order and higher the phases are continuously connected.

The Landau-Ginzburg theory of phase transitions tells us how to infer the order of the transition from the local behavior of the free energy near the critical point. In our case the free energy is the gravitational free energy given by the Hawking-Gibbons action  $I = -\beta F$ , the dimensionless parameter is  $\mu \equiv \mu_\beta$  and  $\lambda$  is the amplitude of the GL mode, so symbolically the perturbation is

$$h \sim \lambda \exp(i k z) h_{GPY} . \quad (3.8)$$

A generic phase transition is of first order as depicted in figure 7. However, in our case  $F$  possesses a certain parity symmetry. We note from (3.8) that  $\lambda$  is complex and

---

<sup>6</sup>The metric signature convention is “mostly plus”.

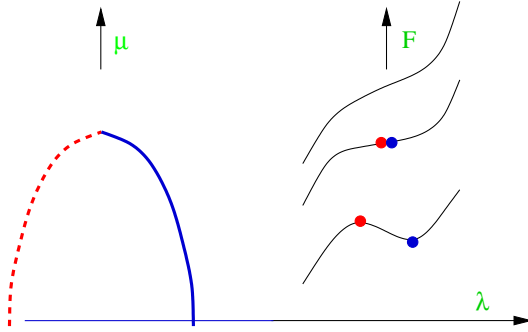


**Figure 7:** The most generic phase transition – first order resulting from a non-zero cubic term in  $F$ . On the right we see a sequence of free energy functions, parametrized by  $\mu$ , with their extrema (phases) highlighted. On the left the phases are extracted into a phase diagram. Stable (unstable) phases are denoted by solid (dashed) lines.

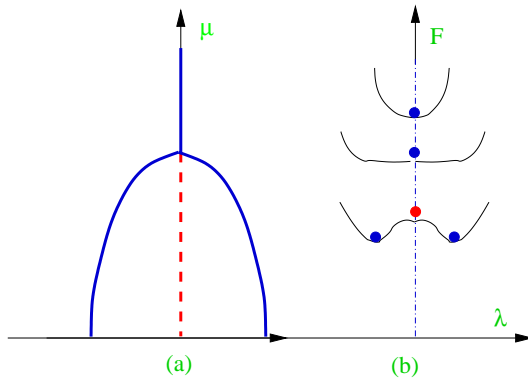


**Figure 8:** For an even free energy the order of transition could be first or higher depending on a sign. In this figure a second order transition (or higher) is caused since the free energy has a minimum at the critical point. Same conventions as in figure 7.

its phase is related to translations in the  $z$  direction. Since the action is invariant under  $z$ -translations we have

$$F = F(\mu, |\lambda|^2), \quad (3.9)$$

and the non-uniform phase spontaneously breaks this symmetry. Actually,  $\lambda$  can be related to the order parameter defined in the previous section, the scalar charge  $b$ . The latter being invariant under  $z$ -translations must be a function of  $|\lambda|^2$  as well. Since they both vanish for the uniform string we conclude that

$$b \propto |\lambda|^2 \quad (3.10)$$

(there is a genericity assumption made here which is confirmed by calculations). From now on, without loss of generality, we consider  $\lambda$  to be real and omit the absolute value notation, so that  $F$  is an even function.

Having a marginally tachyonic mode appear at some critical value  $\mu_c$  means that the quadratic term in  $\lambda$  has a zero at  $\mu_c$ , namely

$$F = F_1(\mu - \mu_c)\lambda^2 + \dots \quad (3.11)$$

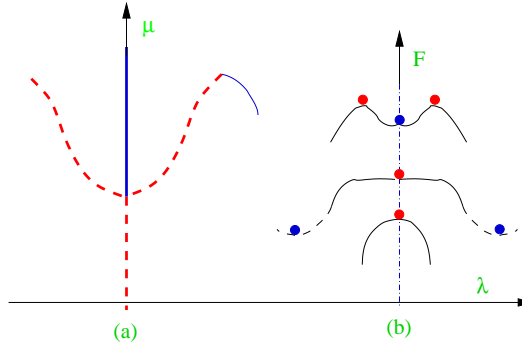


**Figure 9:** An even free energy results in a first order transition if it has a maximum (or more precisely a non-minimum) at the critical point. Same conventions as in figure 7.

where  $F_1$  is some positive constant. Now the Landau-Ginzburg theory suggests to test whether at  $\mu_c$  the free energy has a minimum or not (since  $F$  is even it cannot be monotonous around  $\lambda = 0$ ). If  $F$  has a minimum at  $\mu_c$ , as in figure 8, then for  $\mu < \mu_c$  two stable minima are created close by at small  $\lambda$ , the system will continuously evolve into these new phases and the transition must be second order (or higher). If however  $F$  has a maximum at  $\mu_c$  (or more precisely, a non-minimum), as in figure 9, that means that since  $F$  must be bounded from below there must be some other minimum at some finite value of  $\lambda$ , whose free energy is lower than the uniform string at  $\lambda = 0$ . Therefore the system underwent already a first order transition at some higher value of  $\mu$  where the free energies of both phases were equal.

Therefore Landau-Ginzburg theory instructs us (in our case) to expand

$$F = F_1(\mu - \mu_c)\lambda^2 + F_2\lambda^4 + \dots \quad (3.12)$$

and to determine the sign of  $F_2$ , the quartic coefficient at  $\mu_c$ . Of course if  $F_2$  happens to vanish one needs to compute higher orders, but this did not happen in this system. Actually, so far we neglected all other modes except for the GL mode. When these are brought into consideration one finds it is required to compute first the (quadratic) back-reaction of the GL mode and only then determine the sign of the quartic term in the action.

**Results.** The determination of the order was first carried out by Gubser [38] for the background  $\mathbb{R}^{3,1} \times \mathbf{S}^1$  (see also Wiseman's improvement [39]). Part of the original motivation there was to find a second order phase transition and hence together with it a branch of stable non-uniform strings emanating from the GL point, such as those predicted by [28]. However, the transition was found to be first order. Later Sorkin [27] generalized the method to the backgrounds  $\mathbb{R}^{D-2,1} \times \mathbf{S}^1$  and found a surprising critical dimension

$D \leq 13$	first order
$D \geq 14$	second order .

The critical dimension  $D^* = "13.5"$ <sup>7</sup> is demonstrated in figure 10. In subsection 6.1, “results”, we comment on the relation of this result with the predictions of [28].

<sup>7</sup>Of course dimensions are integral, and the notation means only that the change in the order happens

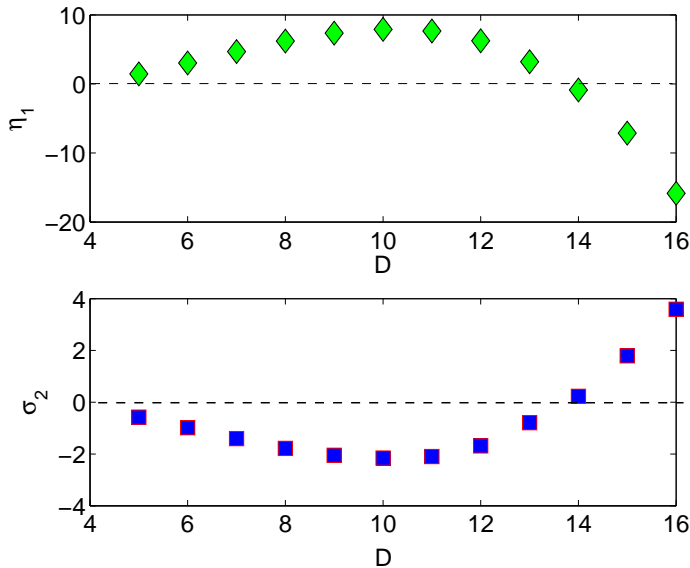


**Figure 10:** The first correction to the mass  $\eta_1$  and to entropy  $\sigma_2$  for the non-uniform string branch emanating from the GL point for backgrounds  $\mathbb{R}^{D-2,1} \times \mathbf{S}^1$  – see [27] for precise definitions. From our general discussion we know that there is only one sign to be determined (that of  $F_2$ ), and indeed the signs of  $\eta_1$ ,  $\sigma_2$  are correlated. At the critical dimension  $D^* = 13.5$  there is a change of sign indicating the transition becomes second order for higher  $D$ . Adapted with permission from [27].

Due to the importance of the critical dimension it is a good idea to develop some intuition about it. First, as discussed around equation (2.12) for high  $D$  the critical GL string is quite “fat” and we expect that the string will not decay (directly) into the black hole, which would be “too big to fit” inside the extra dimension (see also [40] for a similar argument involving  $\mu_S$ , which is defined below). Another indicator comes from comparing  $\mu_{GL}$  with  $\mu_S$  the value of the approximate equal area point:  $S_{St}(\mu_S) = S_{BH}(\mu_S)$  where  $S_{St}$  is the entropy of the uniform string and  $S_{BH}$  is BH area approximated by the small black hole expression. For a first order transition we expect  $\mu_S > \mu_{GL}$  but that holds only for  $D < 12.5$  ( $c = 1$  in figure 11). It is interesting to consider the same estimator for a torus compactification background  $\mathbb{R}^{d-1,1} \times \mathbf{T}^c$  – see figure 11.

**Method.** Gubser’s method [38] was to perturbatively follow the branch of non-uniform strings emanating from the GL critical point. The perturbation parameter is  $\lambda$  the amplitude for the GL mode (3.8), and in order to determine the order of the transition it was necessary to compute some metric functions up to the third order in the perturbation parameter. As we mentioned above, to determine the order there is a somewhat more efficient method, namely it is actually enough to compute only the second order back-reaction and substitute into the quartic part of the action (see appendix A in [29] although this method was not demonstrated in practice yet). However, the longer computation naturally yields additional results not included in the shorter one.

between  $D = 13$  and  $D = 14$ .

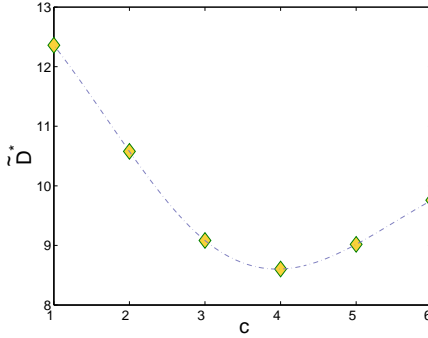


**Figure 11:** An estimator  $\tilde{D}^*$  for the critical total spacetime dimension of (square) torus compactifications, as a function of its dimension  $c$ . Given  $c$  the estimator is the value of  $D$  such that  $\mu_{GL} = \mu_S$  where  $\mu_S$  is the approximate equal area point defined in the text. For  $c = 1$  the estimator  $\tilde{D} \simeq 12.5$  is known to be to small by  $\sim 1$  from the actual  $D^* = 13.5$ . For  $3 \leq c \leq 5$  the indicator is around  $\sim 9$  indicating that second order behavior may be possible in dimensions as low as 10 or 11 where consistent theories of quantum gravity are believed to exist. The needed computation is still under way.

### 3.3 Morse theory

When one turns to consider the question of the end-point for decay, or more generally of finding the phase diagram of all static phases, one is at first discouraged by the lack of any knowledge regarding the non-uniform strings, especially those stipulated to be stable and the big black holes. The most interesting question is to determine the qualitative features of the phase diagram. For that purpose one would need some qualitative tools. Although none were known to the author at the time [29] was written, there was an intuitive feeling that generically a phase persists as the system is “deformed” by changing a parameter, and that the disappearance of a phase should require some special circumstances that are worth elucidating.

Indeed solutions of the Einstein equations are extrema of the gravitational action in the space of metrics, and as such are generically stable under perturbations. The topological theory of extrema of functions is well-known and is called “Morse theory” and it includes the specification of the allowed transitions. <sup>8</sup>

Actually, there is a subtlety in the identification of extrema of the action with solutions of the equations of motion due to gauge (diffeomorphism) redundancy, which we would like to mention. It is certainly true that solutions are extrema of the action. However we wish to consider the action as a function of metrics up to gauge invariance, namely as a function of the gauge-fixed metric. Therefore the extremum equations should be supplemented by the gauge-fixing constraints. Nevertheless, in the case studied in [39] it turns out that the constraints are actually implied by the extremum requirement through a combination of properly chosen boundary conditions and the constraints’ Bianchi identities. It could be that this is a general mechanism.

<sup>8</sup>Some may be familiar with the way Morse theory measures global properties of manifolds (Homology), but here we need a different aspect of the theory – local invariants of extrema under deformation of the function.

**A lightning review of Morse theory** (see section (3.2) of [29] for a somewhat longer introduction). For functions of one variable the ways in which an extrema can disappear are clear

- Annihilation. A maximum and a minimum can coalesce under continuous deformation and disappear into a monotonous function. We call this the basic 1d vertex of “annihilation” – see figure 7.
- Run-away. An extrema of a function  $f(x)$  may run away to infinity either in  $x$  or in  $f$  during a finite range of deformation parameter. In this paper we shall find “annihilation” explanations for changing phases, and thus we will not need to resort to “run-away” explanations, even though they are certainly possible in general.

When one considers a function of several variables,  $f = f(\vec{x})$ , one may get a simple generalization of the basic 1d vertex by adding  $n$  spectating negative directions as well as  $N - n - 1$  positive coordinates, for instance  $f(\vec{x}) = f_0(x_0; \mu) - \sum_{i=1}^n f_i x_i^2 + \sum_{j=n+1}^N f_j x_j^2$ , where  $f_0(x_0; \mu)$  is a 1d function such as the one depicted in figure 7, and  $f_i$ ,  $1 \leq i \leq N$  are positive constants. We obtain

Basic vertex: two extrema with  $n$  and  $n + 1$  negative directions may annihilate.

While for generic extrema the Hessian is non-degenerate, there could be non-generic extrema where  $n$  is not defined. Thus we see a need for a more general vertex. Indeed, Morse theory can be phrased as saying that the most general vertex is a coincidence of several of these basic vertices, thereby justifying the use of the adjective “basic”.

**The conclusion and some reservations.** We see that a stable phase ( $n = 0$ ) is allowed to disappear at the expense of “annihilating” with an unstable phase with one negative mode ( $n = 1$ ). The latter in turn can disappear by annihilating against either  $n = 0$  or  $n = 2$  phases and so one. This is exactly the “*phase conservation rule*” [29] which we were seeking. It sets a strong qualitative constraint on the existence of phases. However, the price to be paid is that all phases must now be mapped out, not only the stable ones.

As shown in figures 8,9 this rule determines the stability of the non-uniform string emanating from the GL point. The question is where could this phase end. From the phase conservation rule we conclude that the simplest way to satisfy it, without requiring any additional phases, is that the non-uniform string phase would annihilate against the black hole phase [29] at a point on the phase diagram that we call “the merger”. Depending on the dimension we either get an unstable black string annihilating with a stable black hole (the string is unstable at least for small non-uniformity and the BH is stable at least when it is small) for  $5 \leq D \leq 13$  or a stable non-uniform string transforming into a stable BH for  $D \geq 14$ .

The statement above, even if intuitive and clear, is not self-evident due to the following reservations. In the next section we will see that Euclidean black hole and strings have *different topologies* and hence their metrics would be expected to live in different, disconnected spaces, and it wouldn’t make sense for phases to move from one space to the

other. Nevertheless, we shall take the prediction above seriously and look whether these two spaces are in some sense glued together. Indeed we shall find a continuous transition (and in finite distance) between the two spaces, which we view as an important confirmation for the consistency of the picture. However, the way in which the spaces are glued is still poorly understood, and the gluing may very well be non-smooth as well as involve the infinite dimensionality of the space of metrics, in which case the validity of the Morse theory argument is not self-evident. At this point, I consider the conclusion above to be essentially correct and justified if not rigorously *a priori* then *a posteriori* by the agreement of the predicted and simulated phase diagrams.

### 3.4 Merger point

In the last subsection we saw how Morse theory makes it plausible that the non-uniform string phase connects with the BH phase. At first it seems that there is a qualitative obstruction for that, namely topology. However, we are familiar with some topology changes such as the flop and the conifold, and one of the surprising results of the research on this system is the emergence of a novel type of topology change called the “merger” transition [29].

**A topology change.** Intuitively the transition from black string to black hole involves a region where the horizon becomes thinner and thinner as a parameter is changed until it pinches and the horizon topology changes. This region is called “the waist” and this process is described in the upper row of figure 12 using the  $(r, z)$  coordinates defined in figure 2. It is important to remember that all metrics under consideration are static and that they change as we change an external parameter, not time. Since the metrics are static we may as well consider their Euclidean versions.

We shall now demonstrate that this merger transition involves a local topology change of the Euclidean manifold. Consider the boundary (of dimension  $D - 1$ ) far away from the pinch point, which is denoted by the dashed line in the figure. Its topology is given by  $\mathbf{S}_\theta^{D-3} \times \mathbf{S}_{r,z,t}^2$  – the angular piece  $\mathbf{S}_\theta^{D-3}$  is obvious while the  $\mathbf{S}_{r,z,t}^2$  is less so. One should remember that not only the angular coordinates but also the time variable is suppressed in the figure. Moreover, in the Euclidean continuation time is compact with its period vanishing exactly on the horizon. *So a circle fibration of Euclidean time<sup>9</sup> over an interval, such that the fibred circle shrinks on the edges exactly produces a topological  $\mathbf{S}^2$ .*

Next we notice that in the black-hole phase the  $\mathbf{S}_\theta^{D-3}$  shrinks completely, while in the string phase the  $\mathbf{S}_{r,z,t}^2$  shrinks. Therefore *the local topology of (Euclidean) spacetime is changing*, not only the horizon topology. Moreover, *the topology change can be modelled by the “pyramid” familiar from the conifold transition* (see the lower row of figure 12). By the nature of topology, in order to change it there must be at least one singular solution along the way (with at least one singular point). The simplest possibility, which is also realized in the conifold is to assume that *the singular geometry is the cone over  $\mathbf{S}^{D-3} \times \mathbf{S}^2$* .

One may wonder whether the local space-time topology change is also accompanied by a change in the global topology. I believe this is the case for the following reason. The

---

<sup>9</sup>which can be seen to be trivial since  $g_{ti} = 0$  for all  $i \neq t$ .

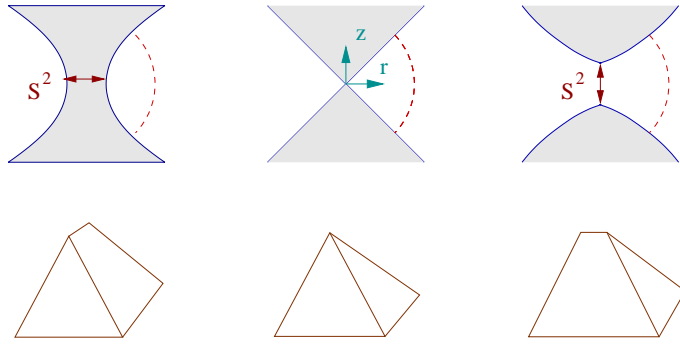


**Figure 12:** The merger transition. Shaded regions are inside the horizon and the dashed line is a boundary far away. The singular configuration is a cone over  $\mathbf{S}^2 \times \mathbf{S}^2$ .

black string solution is contractible to  $\mathbf{S}_\theta^{D-3} \times \mathbf{S}_z^1$  (after contracting the  $r, t$  cigar), and thus its elementary non-contractible cycles are  $\mathbf{S}_\theta^{D-3}$  and  $\mathbf{S}^1$ . For the black hole on the other hand the non-contractible cycles seem to be  $\mathbf{S}_{\chi\theta}^{D-2}$ ,  $\mathbf{S}_{z,t}^2$  and  $\mathbf{S}_z^1$ , which are respectively, the horizon, the symmetry axis  $r = 0$  connecting the poles together with the time fibration and the  $z$  compact dimension. It is seen that there are several differences, for instance, the black hole has a 2d topologically non-trivial cycle while the string does not.

**Cones.** Figure 12 encodes the topology change. But is it really true that this can be realized with Ricci-flat metrics?

It is easy to write down a Ricci flat metric for the singular solution, the cone. Actually this can be done for a somewhat more general cone, the cone over  $\mathbf{S}^m \times \mathbf{S}^n$  with no additional “cost”. The metric is

$$ds^2 = d\rho^2 + \frac{\rho^2}{D-2} [(m-1) d\Omega_{\mathbf{S}^m}^2 + (n-1) d\Omega_{\mathbf{S}^n}^2] , \quad (3.13)$$

where the  $\rho$  coordinate measures the distance from the tip of the cone,  $D = m + n + 1$  is as usual the total spacetime dimension and the constant pre-factors are essential for Ricci-flatness. Note that  $\rho = 0$  is the singular tip of the cone, unless  $m = 0$  (or  $n = 0$ ) when it becomes the smooth origin of  $\mathbb{R}^D$  in spherical coordinates.

In order to exhibit “smooth cone” metrics which approach the singular cone from both sides of the transition one may use the following ansatz

$$ds^2 = d\rho^2 + e^{2a(\rho)} d\Omega_{\mathbf{S}^m}^2 + e^{2b(\rho)} d\Omega_{\mathbf{S}^n}^2 \quad (3.14)$$

with boundary conditions at  $\rho \rightarrow 0$

$$\begin{aligned} a(\rho = 0) &= a_0 \\ b(\rho) &= \log(\rho) \end{aligned} \quad (3.15)$$

such that  $\mathbf{S}^m$  becomes non-contractible while  $\mathbf{S}^n$  joins with  $\rho$  to make a smooth neighborhood of the origin of  $\mathbb{R}^{n+1}$ .

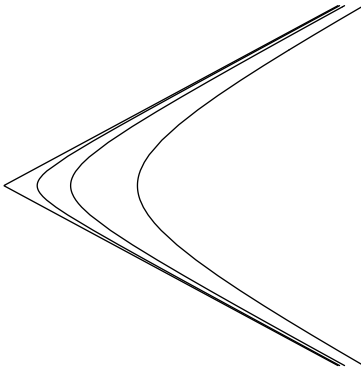


**Figure 13:** A single smoothed cone solution can be scaled down to provide a continuous family of metrics which approach the cone.

Using (A.1) for the Ricci scalar of a fibration and after integration by parts one gets the action for  $a, b$

$$S = \frac{\Omega_m \Omega_n}{16 \pi G_D} \int d\rho e^{m a + n b} \left[ m(m-1)(a'^2 + e^{-2a}) + n(n-1)(b'^2 + e^{-2b}) + 2mn a' b' \right]. \quad (3.16)$$

Einstein's equations are

$$\begin{aligned} a'' &= (m-1)e^{-2a} - m a'^2 - n a' b' \\ b'' &= (n-1)e^{-2b} - n b'^2 - m a' b' \\ 0 &= m(a'^2 + a'') + n(b'^2 + b''). \end{aligned} \quad (3.17)$$

These equations are very similar to the equations encountered in the Belinskii-Khalatnikov-Lifshitz (BKL) analysis of the approach to a space-like singularity (see the recent excellent “Cosmological Billiard” review [5]). Although the general (and often singular) qualitative behavior of these equations as  $\rho \rightarrow 0$  for arbitrary initial conditions was not obtained in [29],<sup>10</sup> it was checked that for the boundary condition above (3.15)  $a(\rho), b(\rho) - \log(\rho)$  can be expanded in a Taylor series around  $\rho = 0$  and the recurrence equations for the Taylor coefficients could be solved without encountering an obstruction.

Once a single smoothed cone solution is available, constructing a full family that approaches the singular cone is a matter of simply rescaling it – as the solution is scaled down more of it approaches the cone (see figure 13).

I would like to stress some of the *assumptions involved* in locally modelling by cones

- The singular solution has a single singular point.

---

<sup>10</sup>One can prove useful theorems for the evolution of the volume factor  $U = e^{m a + n b}$  using the geometric analogue of the “c-theorem” (I thank J. Maldacena for pointing this). From (3.17) we have  $(\log(U))'' = -m a'^2 - n b'^2 \leq 0$  Hence if  $U$  (or equivalently  $\log(U)$ ) is somewhere decreasing it must continue to decrease monotonically. At the same time  $U'' = (m(m-1)e^{-2a} + n(n-1)e^{-2b})U \geq 0$  which together with the previous result guarantees that  $U$  is monotonic.

- Local isometry enhancement – in all the solutions found the  $\chi$  coordinate (see figure 2) conspires with  $t$  to make a round  $\mathbf{S}^2$ . In [29] this local enhancement was argued to be implied by the previous assumption on the nature of the singularity.

A Numeric study [41], limited by numerical resolution, found consistent evidence for this cone structure.

**Tachyons on cones.** It turns out that the cones may have tachyons and that their existence surprisingly depends on a critical dimension  $D_{\text{merger}}^* = 10$  – see [29] and references therein including [42].

The dangerous mode is a function  $\epsilon(\rho)$  which inflates slightly one of the spheres while shrinking the other. The ansatz for the perturbation is

$$ds^2 = d\rho^2 + \frac{\rho^2}{D-2} \left( (m-1) e^{2\epsilon/m} d\Omega_{\mathbf{S}^m}^2 + (n-1) e^{-2\epsilon/n} d\Omega_{\mathbf{S}^n}^2 \right). \quad (3.18)$$

*A priori* one could start with two separate scale functions, one for each sphere, but the constraint relates them as above.

The quadratic part of the action, disregarding an overall constants is

$$I \sim \int \rho^{D-1} d\rho \left[ \frac{2(D-2)}{\rho^2} \epsilon^2 - \epsilon'^2 \right], \quad (3.19)$$

and through the change of variables  $\hat{\rho}^{-1} = (D-2) \rho^{D-2}$  it can be recast to have a canonical kinetic term

$$I \sim \int d\hat{\rho} \left[ \frac{2}{(D-2) \hat{\rho}^2} \epsilon^2 - \epsilon'^2 \right]. \quad (3.20)$$

The eigenvalue problem (eigenvalues of the Lichnerowicz operator) deduced from this action is seen to be in a Schrödinger form

$$\begin{aligned} [-\hat{\partial}^2 + V(\hat{\rho})] \epsilon &= \lambda \epsilon \\ V(\hat{\rho}) &= -\frac{2}{(D-2) \hat{\rho}^2}, \end{aligned} \quad (3.21)$$

where  $\lambda$  is the eigenvalue. Considering potentials of the general form  $V = -c/r^\alpha$  it is well-known that while the classical energy is unbounded from below, the quantum problem may have a ground state as long as the potential is not “too negative”. For instance, for  $\alpha = 1$  we get the Hydrogen atom. More generally the spectrum is bounded from below for  $\alpha < 2$ , while for the critical value  $\alpha = 2$ , which is our concern here, the prefactor  $c$  becomes dimensionless and the potential is conformally invariant. Due to scale invariance the spectrum is constrained to be invariant under positive rescaling of the eigenvalues. Now  $c$  itself exhibits a critical value, namely  $c^* = 1/4$ : the spectrum is bounded from below and actually non-negative only for  $c \leq c^*$  (since the  $E = 0$  solution has no nodes – see for example [43]).

Equating

$$\frac{2}{D-2} = c^* = \frac{1}{4} \quad (3.22)$$

we arrive at [29]

$$D^* = 10 \quad (3.23)$$

which is the critical dimension below which the spectrum is  $(-\infty, +\infty)$ , namely there is a continuum of tachyons, while for  $D > D^*$  it is  $(0, +\infty)$ . Note that  $D^*$  is the total spacetime dimension, and is independent of  $m$  and  $n$  separately. When we wish to distinguish this critical dimension from others we shall denote it by  $D_{\text{merger}}^*$ .

It is interesting to consider also the zero mode for  $\epsilon$ , namely linearized deformations around the cone. From the quadratic action (3.19) we obtain

$$\begin{aligned} \epsilon &= \rho^{s_{1,2}} \\ s_{1,2} &= s_{1,2} = \frac{D-2}{2} \left( -1 \pm i\sqrt{\frac{8}{D-2} - 1} \right). \end{aligned} \quad (3.24)$$

**Some moduli space properties.** As expected from a topology change it lies in finite distance in moduli space. The argument was unpublished so far and here it is supplemented as appendix B. Moreover, the appearance of a kink in the phase diagram at merger was predicted in section (5.3) of [29], and an expanded argument appears in appendix B. The numerics indeed seem to exhibit some sort of a kink – see the next section.

### 3.5 Phase diagrams – predictions and data

We may now assemble all the theoretical input and draw the predicted qualitative form of the phase diagram in the various ranges of dimensions – see figure 14. A diagram like that for  $D \leq 13$  appeared already in [29] (before  $D_{GL}^* = 13.5$  was known). The non-trivial nature of these diagrams is best illustrated by the various other possibilities that were considered in the literature, see for example the six scenarios in [44], section 6.

These are the minimal diagrams consistent with the following results

- The local nature around the critical GL point with its critical dimension  $D_{GL}^* = 13.5$ .
- The merger connection between the string and black hole phases.
- For  $D < D_{\text{merger}}^* = 10$  there are additional tachyons expected as one approaches merger. Since their effect on the phase diagram is unclear at this point, a “black box” was inserted.

Whereas there are infinitely many tachyonic modes in the background of the cone (for  $D < 10$ ), it should be understood that these appear one by one as the merger is approached. This is because away from merger we can think of the cone as being cut off at two scales  $\rho_0 < \rho < \rho_1 \simeq L$ :  $\rho_0$  is the scale of the smoothed-out tip and  $\rho_1$  is a large distance cut-off of order  $L$  since the cone is only a local model. So the system is like a tachyon in a box of size  $\log(\rho_1/\rho_0)$ . If the box is small enough (and assuming Dirichlet boundary conditions) there is no instability, and as  $\rho_0$  decreases and the size of the box grows, more and more tachyonic modes appear. Two speculations for what should be *inside the black box* are shown in figure 15.

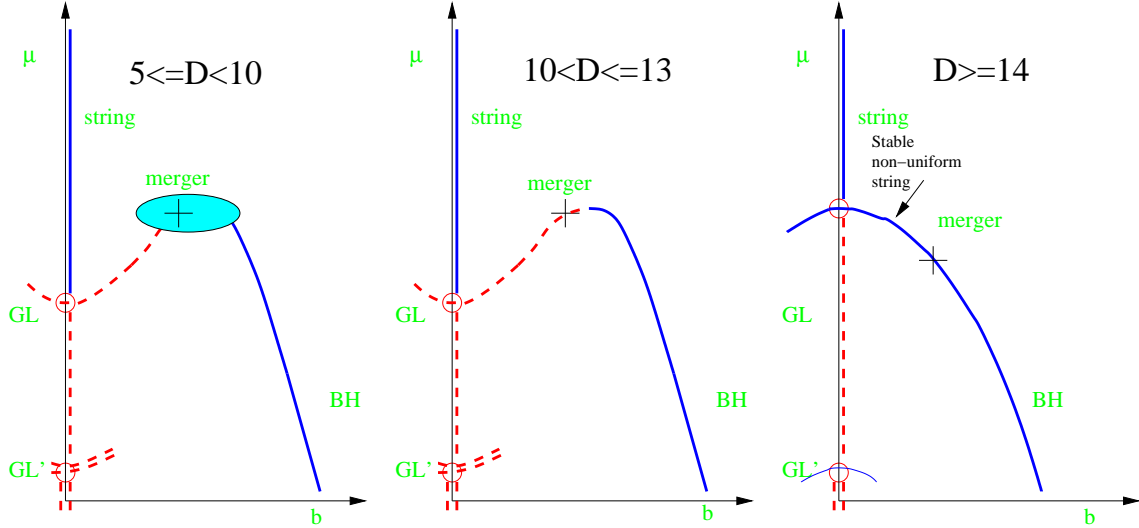


**Figure 14:** The predicted qualitative form of the phase diagram. The vertical axis is the parameter  $\mu_\beta$ , the dimensionless inverse temperature defined in (2.2), and the horizontal axis is the dimensionless scalar charge (see eq. 3.1), which plays the role of the order parameter. Solid (blue) lines denote stable phases and dashed (red) lines denote unstable phases. The “+” denotes the merger point where the black-hole and black-string phases meet in a topology changing transition (of the Euclidean solutions). The “black box” for  $5 \leq D < 10$  is a region of ignorance (see figure 15). Note the dimensional dependence of the qualitative form due to the critical dimensions.

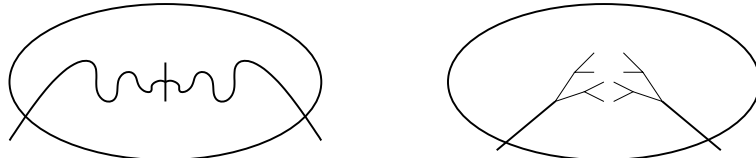


**Figure 15:** Two speculations regarding the contents of the black box around the merger region for  $5 \leq D < 10$  where an infinite number of tachyonic modes are known to appear before merger. On the left each tachyon causes a wiggle of the line according to the basic vertex of Morse theory (subsection 3.3). On the right each tachyon causes a bifurcation of phases, such as at the GL point, resulting in a fractal image.

The critical point  $GL'$  in the figure is there to remind us that each (non-uniform) solution has “*harmonies*” or “*copies*” gotten by considering its period to be  $m L$ ,  $m \in \mathbb{Z}_+$ , rather than just  $L$ . In particular the  $GL$  point has these copies. However, these copies of the phase diagram are decoupled (except for their connection with the uniform string) and therefore there is no point in drawing them. See also [44].

**Numerical data.** One of the joys of this problem is the feedback between theory and numerics, which is in many ways like the classical feedback between experiment and theory which we sorely miss.

Recently the numerical determination of the phase diagram in 6d was all but completed [22] – see figure 16. A visualization of the merger transition through embedding diagrams

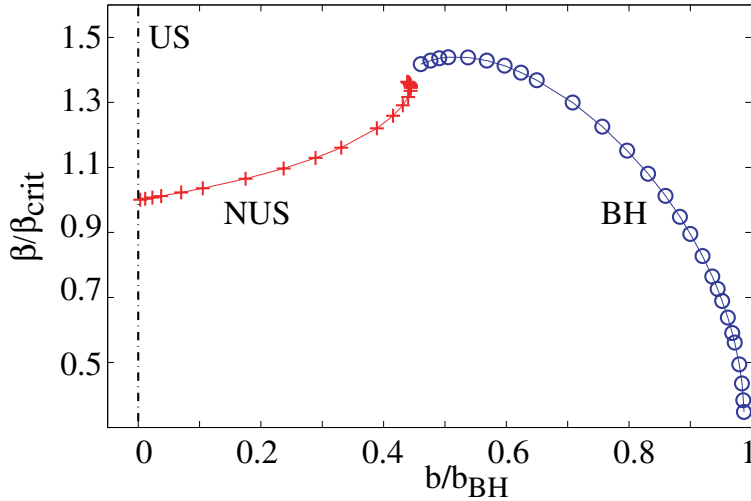


**Figure 16:** Numerical data for the phase diagram in 6d. “US” denotes the uniform string branch, “NUS” denotes the non-uniform string branch (data from [39]) and “BH” is the black hole (data from [22]). Axes conventions are the same as in figure 14 (only the scalar charge is in units of mass rather than temperature). Adapted with permission from [22].

is shown in figure 17.

We see perfect agreement with the predicted diagram, figure 14 with  $D = 6$ , especially regarding the prediction for a “merger” connection between the black hole and the string phases, and the absence of a stable non-uniform phase (predicted by [28]). We view this as a vindication of the picture presented here. Additional interesting features of the numeric figure are a kink at merger,<sup>11</sup> perhaps related to the predicted kink (see the last paragraph in the previous subsection), and the location of the merger at roughly a local maximum on the diagram.

These diagrams were obtained by combining data from two different simulations - one for non-uniform strings [39] and one for the black holes [22], see also [20, 21] for previous work. More details on the challenges overcome in performing these simulations appears in the next section.

## 4. Obtaining solutions

In the previous section we examined the qualitative features of the phase diagram. Now we turn to the more quantitative aspects, those required in order to obtain solutions for static black objects.

### 4.1 2d gravito-statics

**Counting degrees of freedom.** The most general metric which is static<sup>12</sup> and spherically

<sup>11</sup>However, the geometry of the horizon and axis seems to merge rather smoothly.

<sup>12</sup>“Static” means by convention invariance not only under time translations but also under time reversal, so that  $g_{ti} = 0$ ,  $i \neq t$ .

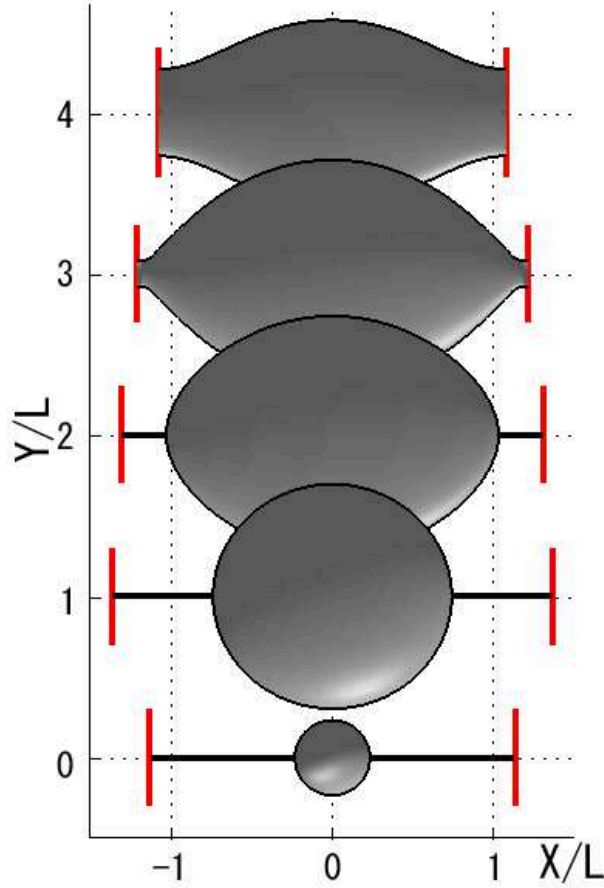


**Figure 17:** Embedding diagrams for a sequence of event horizons in 6d, starting with non-uniform strings (top, data from [39]) and passing through the merger transition to black holes (bottom, data from [22]).  $X$  is the compact dimension and  $Y$  is the radial direction. Note that although the asymptotic size of the extra dimension,  $L$ , is kept fixed, the “proper” size (for embedding purposes) changes. Reproduced with permission from [22].

symmetric is

$$ds^2 = e^{2A} dt^2 + ds_{(r,z)}^2 + e^{2C} d\Omega_{D-3}^2, \quad (4.1)$$

where all functions are defined on the  $(r, z)$  plane,  $ds_{(r,z)}^2$  is an arbitrary metric on the plane and since the metrics are static we might as well work with Euclidean signature.

Altogether the problem is defined in the 2d  $(r, z)$  plane and the field content is the metric and two scalars  $A, C$ . That means that we can write down a 2d action for these fields without loosing any of the equations of motion. The action is

$$S = \frac{\beta L}{4G_D} \int dV_2 e^{A+2C} \cdot [R_2 + (D-3)(D-4) e^{-2C} + (D-3)(D-4) (\partial C)^2 + 2(D-3) (\partial A)(\partial C)] \quad (4.2)$$

where  $R_2$ ,  $dV_2 := \sqrt{g_2} dr dz$  are the 2d Ricci scalar and volume element (see appendix A for useful formulae to determine this and related actions). The total number of fields is 5.

Two fields may be eliminated by a choice of coordinates in the plane which leaves us with three fields. As we proceed we shall review some of the gauges that were used.

If we formally compute the number of “dynamic” or “physical” degrees of freedom we get a total of  $-1 + 2 = +1$ :  $-1$  is for the metric and  $+2$  is for the two scalars. So far nobody succeeded in reducing the problem to a single field, and it is not clear whether that is possible or not, but there is a clever ansatz due to Harmark and Obers which reduces the problem to two fields [45], (see (4.10,4.12) and thereabout) . Morally speaking, one may hope that the equations for the three fields, if not reducible to a single field, could at least be separated such that first one solves two equations for “diffeo gauge fields” and only then a single equation is solved for the “physical field”.

Note that if we relax the static requirement the number of degrees of freedom increases – see subsection 4.3.

**Constraints and boundary conditions.** Today numerical relativists perform full 3+1 dimensional simulations with some success. One would think that simulating a static problem, namely “*gravito-statics*”, would be well-understood by now, but this turned out not to have been the case. The main conceptual hurdle which was necessary to cross was the treatment of constraints and boundary conditions. This problem was solved by Wiseman in the 2d case [39], as we now describe.

Since classical gravito-statics is equivalent to *electro-statics* it is useful to recall the method there. In electro-statics one wishes to find the electro-static potential  $\Phi(x)$  defined over some domain, satisfying

- The Poisson equation

$$\Delta\Phi = -4\pi\rho, \quad (4.3)$$

where  $\rho$  is the given charge density distribution

- Boundary conditions: Dirichlet, Neumann or some mix.

A successful numerical implementation of this problem is *the relaxation method*. This method is very physical in the sense that it is quite close to describe the way in which an excited field settles down or “relaxes” with time to a static solution. In the relaxation method one chooses a grid, consisting of points  $x_i$ , and then one starts with an initial field configuration  $\Phi^{(0)}(x_i)$  which satisfies the boundary conditions. At each step  $\Phi$  is modified to create a sequence  $\Phi^{(j)}$  which converges to the solution as  $j \rightarrow \infty$ . The modification at each step is according to a local rule, a discretization of the Laplacian, which essentially sets

$$\Phi^{(j+1)} = \langle \Phi^{(j)} \rangle_{\text{neighbors}} \quad (4.4)$$

namely each interior point is assigned the average over its neighbors. Actually, one can introduce a “relaxation speed” parameter,  $\omega$ , defined by

$$\begin{aligned} \Phi^{(j+1)} &= \Phi^{(j)} + \omega \Delta\Phi \\ \Delta\Phi &= \langle \Phi^{(j)} \rangle_{\text{neighbors}} - \Phi^{(j)} \end{aligned} \quad (4.5)$$

such that  $\omega = 1$  corresponds to the rule (4.4), while  $\omega > 1$  is called “over-relaxation” and  $\omega < 1$  is called “under-relaxation”. Clearly, the solution is a fixed point of the process, irrespective of the value of  $\omega$ . Its importance lies in changing the convergence properties. For some interval of  $\omega$  containing  $\omega = 1$  the process is guaranteed to converge since at each step the energy is reduced and the solution is a unique and global minimum of the energy. In this range  $\omega$  may be adjusted for convergence speed.

Similarly to electro-statics, General Relativity allows for relaxation. In our case there are 5 equations of motion, and after fixing the gauge the equations are split to 3 equations of motion and 2 constraints (“gauge fixing constraints”). Wiseman chose essentially the “conformal” gauge

$$ds^2 = e^{2A} dt^2 + e^{2B} (dr^2 + dz^2) + e^{2C} d\Omega_3^2 \quad (4.6)$$

for the 6d problem. However, I expect that the following description of the constraints and boundary conditions (b.c.) holds also for more general gauges. The 3 equations of motion are elliptic of the form

$$\Delta X = Src \quad (4.7)$$

where  $X$  is any of the fields  $A, B, C$ ,  $\Delta = \partial_{zz} + \partial_{rr}$  is the flat space Laplacian, and  $Src$  are some non-linear functions of the fields. As such we would like to subject them to relaxation with some b.c. at infinity and at the horizon. Normally 3 elliptic equations require three boundary functions as data. However, the analogy with electro-statics leads us to expect the b.c. to consist of a single function. So the question is how to determine the b.c. Another problem is how to guarantee that the remaining two constraints, which are hyperbolic in this case, are satisfied as well.

The problems of b.c. and constraints are solved simultaneously by noting the constraints’ Bianchi identities. In this specific ansatz the constraints are  $G_{rz}$  and  $G_{rr} - G_{zz}$ , where  $G$  is the Einstein tensor. The Bianchi identities are

$$\begin{aligned} \partial_r(g G_z^r) + \partial_z \left( \frac{g}{2} (G_r^r - G_z^z) \right) &= 0 \\ \partial_z(g G_z^r) - \partial_r \left( \frac{g}{2} (G_r^r - G_z^z) \right) &= 0, \end{aligned} \quad (4.8)$$

where  $g = \det g_{\mu\nu}$  and one uses the Einstein tensor with mixed upper and lower indices. These are Cauchy-Riemann equations and hence

$$G := g \left( G_z^r - \frac{i}{2} (G_r^r - G_z^z) \right) \quad (4.9)$$

is *analytic in the  $r + iz$  variable*. For an analytic function to vanish in a domain, we know that it is exactly enough to impose that its real part vanishes on the boundary and that its imaginary part vanishes at a point. Alternatively, one may impose the boundary constraint  $\text{Re}(e^{i\alpha} G) = 0$  for any constant  $\alpha$  together with  $\text{Im}(e^{i\alpha} G) = 0$  at a single boundary point. It turns out that these boundary conditions chosen by the constraints’ Bianchi identities, do not only guarantee the constraints but are also exactly sufficient for the elliptic problem. Note that altogether the b.c. consist of a single function, as expected from the analogy with electro-statics (plus a function at one point), and that there is some freedom in specifying the b.c. (such as choosing  $\alpha$ ) which is analogous to the choice of Dirichlet/ Neumann.

Since the Cauchy-Riemann equations are special to 2d it is not obvious how to generalize this structure to higher dimensions gravito-statics, which would occur for higher dimensional compact manifolds. One may speculate though, that the general rule is the same as the last highlighted sentence.

Another issue of boundary conditions, which is dealt with in the conformal gauge (4.6), is fixing the boundary. In GR, due to the dynamic nature of the metric one cannot anticipate the final location of the horizon. However, it is normally best for numerics to fix the location of the horizon in coordinate space. The conformal gauge allows for analytic coordinate change as residual gauge. It was shown that this freedom exactly suffices in order to fix the horizon to be say, a circle of size  $\rho_h$  in the  $(r, z)$  plane, by writing down elliptic equations for the coordinate transformation [46]. In these coordinates  $\rho_h$  is a free parameter that determines the size of the black hole.

### Harmark-Obers coordinates

By choosing the coordinates with some physical logic Harmark and Obers found an ansatz with 2 rather than 3 fields [45]. The ansatz was constructed for black hole solutions, and it explicitly fits the uniform string but it was not used so far for non-uniform black strings and we comment on this later in this subsection.

[45] start by defining orthogonal coordinates  $(R, v)$  over the  $(r, z)$  plane such that they interpolate between spherical coordinates near the origin and cylindrical coordinates asymptotically. To that purpose  $R$  was defined through  $H(r, z)$ , the Newtonian potential for a point source at the origin (see figure 18)<sup>13</sup>, by

$$\left(\frac{R_0}{R}\right)^{d-3} = H. \quad (4.10)$$

$v$  is defined to be an orthogonal coordinate of period  $2\pi$  and it can be parametrized such that near the origin it approaches  $\chi$  (see figure 2) while asymptotically it approaches  $z$ . This is achieved by the system

$$\begin{aligned} \partial_r v &= k r^{d-2} \partial_z H \\ \partial_z v &= -k r^{d-2} \partial_r H, \end{aligned} \quad (4.11)$$

where  $k$  is some constant and the system is integrable since  $H$  is harmonic. We see here that this construction is special to 2d, and it is not clear whether it can generalized to higher dimensions.

The  $(R, v)$  plane is drawn in figure 19. It is a semi-infinite cylinder with one marked point (denoted by  $x$ ), which is  $(r, z) = (0, L/2)$ , where the equipotential surfaces turn from spheres to cylinders and the differential of the transformation from  $(r, z)$  to  $(R, v)$  vanishes. In these coordinates  $R_0$ , the location of the horizon, is a free parameter that determines the size of the black hole, while the location of the marked point remains fixed at some  $R_1$ . As the black hole grows  $R_0$  reaches  $R_1$  and from then on the same equations should generate string solutions rather than BHs (for some appropriate boundary conditions).

---

<sup>13</sup>[45] find an explicit expression for  $H$  by separating variables and expressing the radial functions in terms of modified Bessel functions of the second kind.

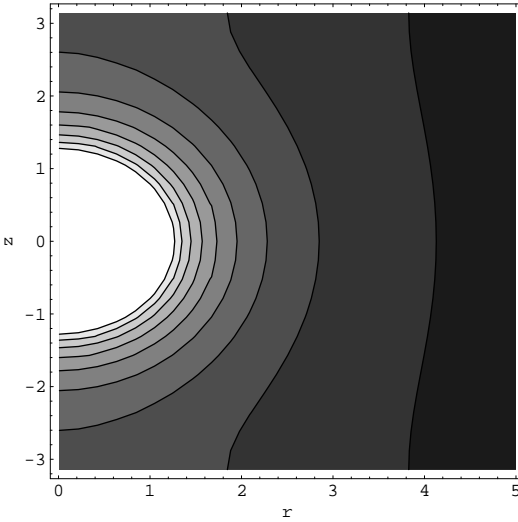


**Figure 18:** The equipotential lines of the Newtonian potential around a point-like source in 5d drawn in the  $(r, z)$  plane. Note the change in their topology from spheres to cylinders.

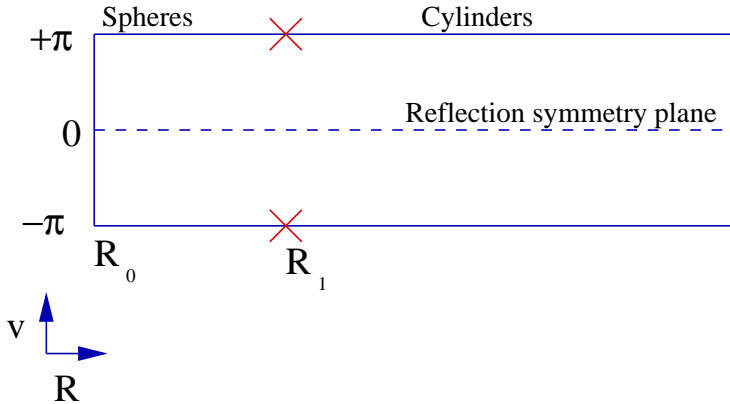


**Figure 19:** The Harmark-Obers coordinates  $R, v$  [45].  $R$  is a function of the Newtonian potential and  $v$  is periodic with period  $2\pi$ . The  $x$  marks the point  $(R, v) = (R_1, \pi)$  which is a singular point of the coordinate transformation. For  $R < R_1$  equal- $R$  surfaces are spheres while for  $R < R_1$  they are cylinders. The size of the black hole is changed by adjusting  $R_0$ .

In the  $(R, v)$  coordinates it turns out that two fields  $A, K$  suffice (rather than three), according to the following ansatz

$$ds_{d+1}^2 = f dt^2 + \left(\frac{L}{2\pi}\right)^2 \left[ f^{-1} A dR^2 + \frac{A}{K^{d-2}} dv^2 + K R^2 d\Omega_{d-2}^2 \right] \quad (4.12)$$

where

$$f = 1 - \frac{R_0^{d-3}}{R^{d-3}}. \quad (4.13)$$

The justification for this ansatz was demonstrated (in 6d) [47] by showing that for any solution the equations for a change of coordinates to the ansatz (4.12) are self-consistent. The proof was then generalized in [44] to any dimension. Another way to see that reduction is to write a fully general ansatz by adding a third field  $C$ , say as the coefficient of  $dv^2$ , and then one finds that the  $G_{tt}$  constraint gives an algebraic relation between the three fields [48]. Yet, it is not clear how the reduction of fields could have been anticipated and whether there are other ansatzs with this same property.

A further reduction is possible, expressing  $A$  in terms of  $K$  and its second derivatives (eq (6.6) of [45]). However, this may not be useful since it would make the equations of order higher than second, and hence unamenable to relaxation (actually even the equations for both  $A, K$  were not brought to relaxation form so far, but that should be possible).

## 4.2 Numerical issues

We turn to a brief overview of the numerical implementation issues of our gravito-statics problem. The first simulation of the system was [39] which found the correct prescription for b.c. and constraints and applied it to obtain solutions for non-uniform strings including highly non-uniform ones very close to the merger point. That work benefitted from insights gained from works on the “black hole on a brane” problem such as [49]. A simulated black hole on a brane appeared in [46] while the first simulation for caged BHs appeared simultaneously in [20] (5d) and [21] (6d). However, due to convergence problems large black holes were not possible to obtain. These problems were largely overcome in [22] (5d & 6d) whose figures 16,17 summarize the state of the art.

**Implementation.** The most important decisions for implementing the numerics are the choice of coordinates, fields and grid. So far *the coordinates and fields* were chosen in accordance with the conformal gauge (4.6), with variations intended to extract the singular and asymptotic behavior for smoother numerics. For example, the ansatz used in [39] for 6d strings was

$$ds^2 = \frac{r^2}{G_5 m + r^2} e^{2A} dt^2 + e^{2B} (dr^2 + dz^2) + e^{2C} (G_5 m + r^2) d\Omega_3^2. \quad (4.14)$$

In [20] the implementation proved to be very sensitive to a redefinition of fields, for some unclear reason, the main obstacle being a simple linear redefinition of fields of the form  $B' = B + C$ ,  $C' = B - C$ . The more efficient Harmark-Obers coordinates were not implemented so far and it would be interesting to do so.

When choosing a grid one should consider the following factors: the number of nearest neighbors for each point, the density of points and multi-grid issues. Hexagonal lattices are particularly suited for the solution of the Laplace equation in 2d, because one can first use some relaxation method just to distribute the grid points according to some precision requirements, and then weights for the discretized Laplacian are uniquely determined from the points location. However, for convenience all simulations so far involved square grids and the density of points was adjusted by using the mapping from grid space to coordinate space. For instance in [20] two grids were used: in the near zone the grid was evenly

spaced in  $\rho$  and  $\cos(\chi)$  (see figure 2 for coordinate definition) while in the asymptotic zone it was evenly spaced in  $\log(r), z$ . The need for two grids came from the need for different densities of points in the two regions. The price to pay is in the complexities of grid matching. Another grid tool employed in [20] was the “multi-grid” where the problem was relaxed successively on finer and finer grids, in order to accelerate convergence.

Another, less critical choice, is the choice of discretization of the differential operators.

**Convergence.** Having implemented the numerical scheme, one typically presses “enter” and prays for convergence. To achieve it one is free to use the “convergence speed” parameter  $\omega$  (4.5). Often this does not suffice and we enter the domain of black magic. One difficult problem that arose from an innocent redefinition of the fields was already described.

Another issue involves non-convergence as a result of problems near the exposed  $r = 0$  axis (so it does not apply to strings). This problem is known to be solved effectively by the following “Wiseman trick” [49]. The field  $B$  appears in source terms which are sensitive to errors near the exposed axis and generate instabilities. To cure that one replaces  $B$  by a numerically distinct variant,  $B2$ , which is meant to be more accurate than  $B$  near the axis and is gotten by integrating a constraint from the axis outward.

More generally, one expects to have a relation between physical stability of a solution and convergence. However, the method converges nicely for non-uniform strings which are believed to be unstable. The convergence is the result of boundary conditions at the horizon which force the solution to be non-uniform and which perhaps can be described as exerting some “pressure” which stabilizes the string also in the physical sense. It would be nice to understand this issue better.

**Tests.** The results of the simulations must be tested. The following tests were employed

- Convergence.
- Constraints.
- Integrated first law.

This law (3.7) relates  $m, \tau$  which are measured at infinity with  $\beta, S$  measured at the horizon. As such it provides a strong overall test of the numerics, and it is satisfying to find that it holds. However, as the first law is proven using integration by parts, and for that the equations of motion are sufficient, it is not sensitive to violations of the constraints.

- Comparison with analytic results.

Some analytic results for small black holes (see subsection 4.4) allow testing of the numerical data. *The satisfying agreement is demonstrated in figures 20, 21, 22, 23* taken from [20]. In all figures the size of the BH is measured by  $x := 2\rho_h/L$  where  $\rho_h$  is the horizon radius in conformal coordinates and this “numerical” definition of  $x$ , valid in this subsection, should not be confused with a different “analytic” definition

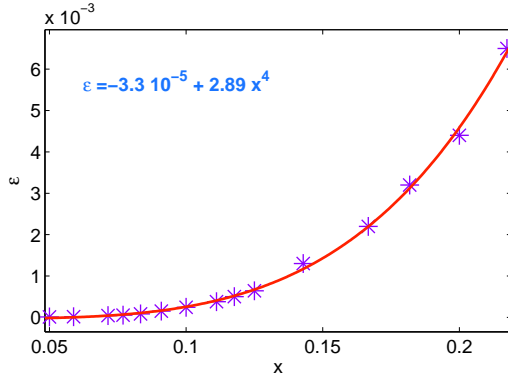


**Figure 20:** 5d Black hole eccentricity as a function of black hole size. Simulation and analytic expression agree. The eccentricity  $\epsilon$  is defined in (4.23). Reproduced from [20].

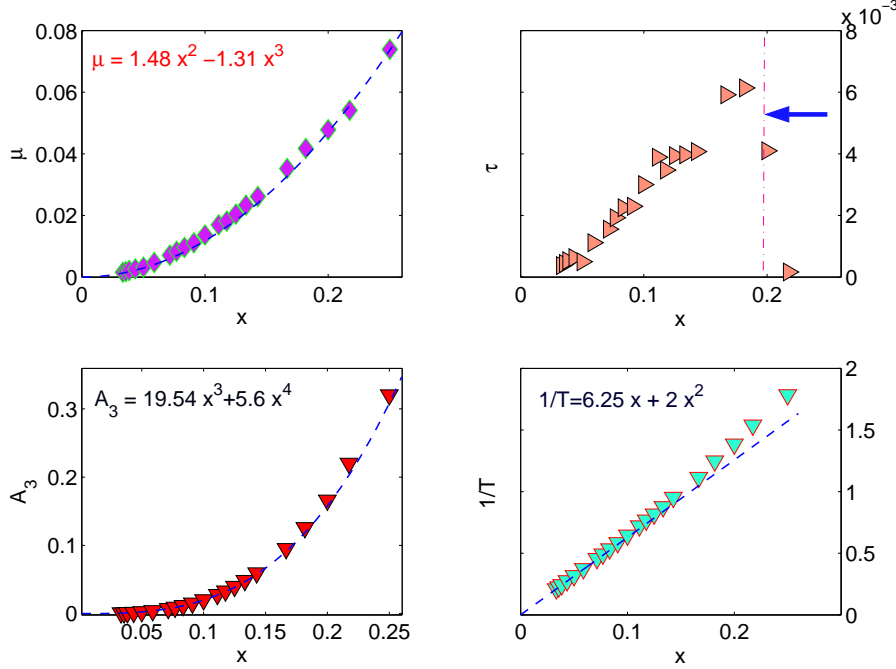


**Figure 21:** Thermodynamic quantities,  $\mu$ ,  $\tau$ ,  $A_3$ ,  $1/T$  which are the mass, tension, area and inverse temperature, respectively, of a 5d black hole as a function of its size. Simulations and analytic expressions agree, except for the tension results which are less reliable. Reproduced from [20].

of the small parameters  $x$  valid in subsection 4.4. Stars, diamonds or triangles represent actual simulation results while the curve represent smooth interpolations which coincide with the theoretical predictions of [17] within the simulation precision.

### 4.3 Time evolution

As remarked in subsection 2.4, “issues”, the time evolution of the unstable system raises deep questions regarding singularities. Thus there is ample motivation for a dynamical numerical simulation. On the other hand, we expect any such simulation to crash before

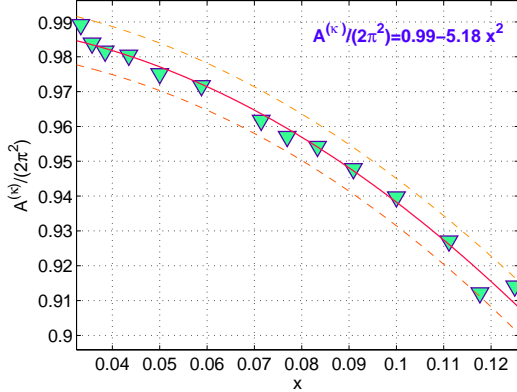


**Figure 22:** The area in units of the surface gravity,  $A^\kappa$ , as a function of 5d black hole size. This quantity measures a correction to the temperature due to the non-zero potential at the origin from the image BHs. Simulation and analytic expression agree. Reproduced from [20].

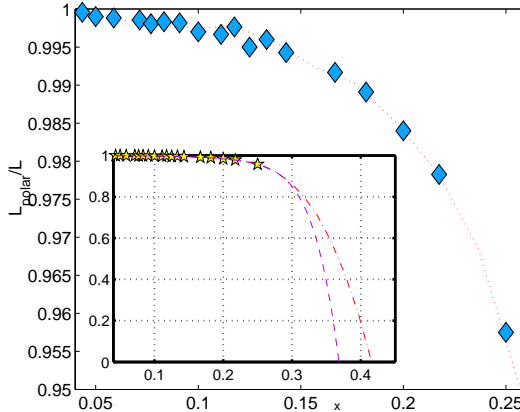


**Figure 23:** The inter-polar distance (going around the compact dimension), defined in figure 28, as a function of black hole size in 5d. Simulation and analytic expression agree. Reproduced from [20].

the singularity is reached. So in order to achieve progress it is probably necessary to have a theoretical local model for the time evolution, which could then be tested and supported by a numerical simulation.

Thus far there has been a single time evolution simulation: [50] simulated the decay of a sub-GL uniform string in 5d. The main features of the evolving spacetime can be read from figure 24. The initial configuration is an unstable string of radius  $r_0$  on top of which the unstable perturbation grows in time. In the region where the horizon moves radially inward (the “waist”) the collapse is fast, stretching at the same time in the  $z$  direction (growing  $g_{zz}$ ) until the minimal (areal) radius reaches about  $0.15 r_0$  when the grid stretching is so large that the simulation cannot proceed. In the region where the horizon grows (the “hip”) the metric approaches the metric of a 5d BH with a comparable mass, so that the maximal (areal) radius at the horizon is about  $2 r_0$ .

The author of this review interprets these results as *strong evidence against the forma-*

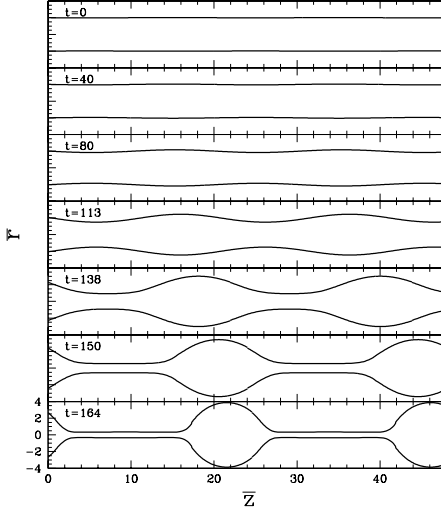


**Figure 24:** A time sequence of embedding diagrams for the event horizon of a decaying black string in 5d, from a numerical time evolution. Initially, the string is nearly uniform (top), and by the time the simulation comes to a stop due to grid stretching (bottom), the horizon becomes that of a black hole with a thin pipe connecting the poles (going around the extra dimension). Reproduced with permission from [50].

*tion of a stable non-uniform string end-state.* The authors of [50] are much more careful and would only say that the results “are not inconsistent with Gregory and Laflamme’s conjecture that the solution bifurcates into a sequence of black holes ... [On the other hand it is] not necessarily inconsistent with [28]... At the same time, a continuation of the observed trend would argue against achieving a stationary solution with a mild dependence on the string dimension”.

In light of the critical dimension  $D^* = “13.5”$  it would be very interesting to run the simulation again for a range of dimensions, and to test/ confirm that for  $D \geq 14$  the unstable string changes a little and settles down to a slightly non-uniform string.

**Method.** Let us count the number of degrees of freedom, which is of course larger than in the static case. The domain is the 3d space parametrized by  $(r, z, t)$  and the fields are the metric and the scalar which is roughly  $g_{\theta\theta}$  or  $C$  in (4.1). The total number of fields is 7. After choosing some gauge in the 3d domain the number of fields reduces to 4 (compared to 3 in the static case). Finally, the “physical” number of degrees of freedom is a total of  $0 + 1 = 1$  (just like the static case): none for the graviton and +1 for the scalar.

The most general time-dependent metric is

$$ds^2 = (-\alpha^2 + \gamma_{AB}\beta^A\beta^B)dt^2 + 2\gamma_{AB}\beta^A dx^B dt + \gamma_{AB}dx^A dx^B + \gamma_\Omega d\Omega^2 , \quad (4.15)$$

where  $x^A = (r, z)$ , and  $d\Omega^2$  is the 2-spherical line element with coordinates chosen orthogonal to the  $t = \text{constant}$  congruences (hence there is no shift corresponding to angular directions). All metric components in (4.15) are defined in the 3d domain. [50] choose the gauge

$$\alpha = \alpha_{St}$$

$$\begin{aligned}\beta^z &= 0 \\ g_{\theta\theta} &= r^2,\end{aligned}\tag{4.16}$$

where the string metric function is read from the ingoing Eddington-Finkelstein form

$$ds_{St}^2 = -(1 - 2M/r) d\tilde{t}^2 + 4M/r dr d\tilde{t} + (1 + 2M/r) dr^2 + dz^2 + r^2 d\Omega^2. \tag{4.17}$$

They also comment that “In a preliminary version of our code, we also required that  $\beta^r = \beta_{\text{BS}}^r$ . This, however, caused a coordinate pathology to develop at late times during the evolution of unstable strings—specifically, some regions of the horizons approached a zero coordinate-radius, while maintaining *finite* proper radius.” Thus the condition on  $\beta^z$  was replaced by one on  $g_{\theta\theta}$ .

Another hurdle turned out to be the boundary conditions at infinity. To eliminate cut-off problems spatial infinity was brought to a finite point by replacing  $r$  by  $r/(r + 1)$ .

#### 4.4 Analytic perturbation method

While we do not know to write the black hole metric in closed form, metrics for small black holes can be well-approximated everywhere: for  $\rho \ll L$  the  $D$  dimensional black hole is a good approximation, while for  $\rho \gg \rho_0$  ( $\rho_0$  is the Schwarzschild radius) the Newtonian approximation is good. Moreover the two approximations have an arbitrarily large overlap in the small black hole limit. Therefore, one expects that the black hole metric can be systematically expanded in a perturbation series with a small parameter being  $x := \rho_0/L$ .<sup>14</sup> The general procedure and first order results were given in [17] (and pre-announced in [19]). A different, one zone approximation was given in [16]. Finally, very recently the full second order was obtained in 5d in [18].

The objectives here are to

- Provide tests for numerics.
- Extrapolate to the phase transition region.

**Method.** It is not possible to use the usual perturbation method since the domain of coordinates changes with  $x$ , and since we do not have a zeroth order solution. However, one can use the well-known technique of “matched asymptotic expansion”. In [17] this technique was applied by defining two zones: an “asymptotic zone” and a “near horizon zone” (see figure 25), which have a large overlap in the limit  $x \rightarrow 0$ . The metric is solved perturbatively in each zone, with boundary conditions coming from matching with the other zone. The need for matching produces an intricate (and dimension dependent) pattern of crossings between the two zones – “the perturbation ladder” – see figure 26. Effectively the gravitational field produced by the images changes the shape of the BH, or its mass multipoles, and that in turn back-reacts and changes the field multipoles. This procedure, which being static is much simpler than the usual dynamic matched asymptotic expansion, was termed “*a dialogue of multipoles*”.

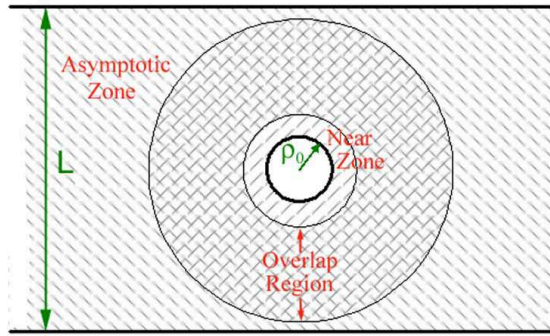


**Figure 25:** The metric for small black holes can be obtained through matched the a “dialogue of monopoles” matched asymptotic expansion. The two zones are the asymptotic zone  $\rho \gg \rho_0$  and the near zone  $\rho \ll L$ . The smaller the black hole the larger is the overlap region between the two zones.

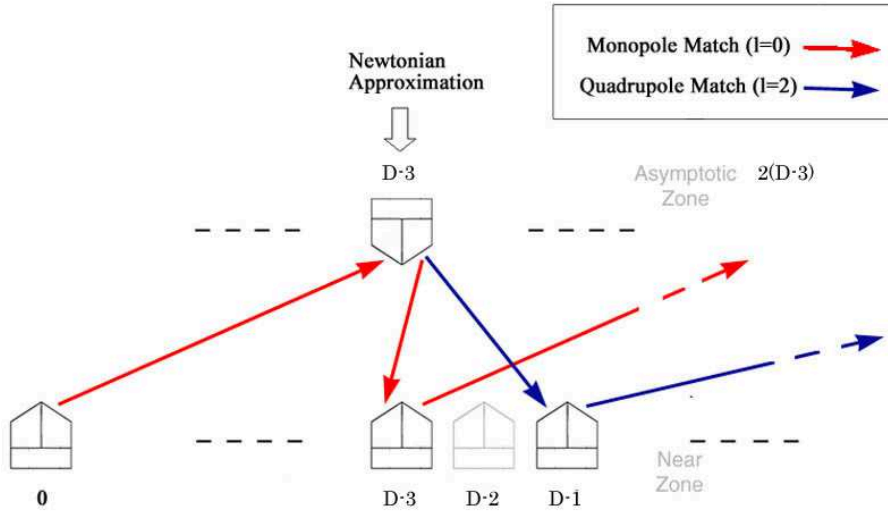


**Figure 26:** The “perturbation ladder” for the “dialogue of monopoles” matched asymptotic expansion. The upper row depicts the asymptotic zone and the lower row the near zone. Each box denotes a certain order in the perturbation series – in the asymptotic zone one counts orders of  $\rho_0$  and in the near zone orders of  $L^{-1}$ . The arrows denote the flow of information between the two zones, in supplying boundary conditions through matching. The figure shows the general pattern for an arbitrary spacetime dimension  $D$ . Reproduced from [17].

<sup>14</sup>This “analytic” definition of  $x$ , valid in this subsection, should not be confused with a different “numerical” definition of the small parameters  $x$  valid in subsection 4.2.

The zeroth order in the asymptotic zone is flat space with a compact dimension and the origin removed, while in the near zone it is the Schwarzschild black hole, with the periodicity  $L$  being far away and invisible. The first order analysis in the asymptotic zone is easy – it is just the Newtonian potential. However, the first correction to the near zone requires more work – it is a generalization to higher  $D$  of the well-known paper by Regge and Wheeler [51]. The metric is given in terms of a single function  $E = E(\rho, \chi)$  which determines the metric. After separation of variables into  $E_l(\rho)$  it satisfies a “master equation”

$$\frac{D^2 E}{dX^2} + \left( \frac{2}{X} + \frac{1}{X-1} - \frac{1}{X-w} \right) \frac{dE}{dX} - p(1+p) \frac{X + (D-4)w}{X(X-1)(X-w)} E = 0 \quad (4.18)$$

where  $l$  is the angular momentum and

$$\begin{aligned} X &:= (\rho/\rho_0)^{D-3} \\ w_{l,D} &:= -\frac{D-2}{(l-1)(l+D-2)} \\ p_{l,D} &:= \frac{l}{D-3} . \end{aligned} \quad (4.19)$$

There are four singularities, (so it is a “Heun equation”, by definition) at  $0, \rho_0, \infty$  and at  $w$ , but the latter is “non-physical” and can be eliminated, and since there are 3 remaining singularities the solutions can be expressed in terms of hyper-geometrical functions. These results were first obtained by [52] by a somewhat different method.

In [16] an alternative method was given employing a single patch, and using the efficiency of Harmark-Obers coordinates [45]. There a “first order” approximation is given, and I expect that the method could be developed to a full perturbation series by successively improving a suitably chosen initial guess. It has the advantage of using only a single zone, and doing away with matching. However, the method depends on the choice of initial guess, and unlike the previous method, the differential operator to be inverted would probably change at each order.

**Results.** In 5d we now have the second order metric [18] (second order for arbitrary  $D$  is to appear in [53]), from which the following thermodynamics were deduced

$$\begin{aligned} S &= \frac{\pi^2 L^3}{2G_5} \tilde{\epsilon}^{3/2} \left( 1 + \frac{\pi^2 \tilde{\epsilon}}{8} + \frac{\pi^2 \tilde{\epsilon}^2}{384} \right) \\ T &= \frac{1}{2\pi\mu} \tilde{\epsilon}^{3/2} \left( 1 - \frac{5\pi^2 \tilde{\epsilon}}{24} + \frac{43\pi^4 \tilde{\epsilon}^2}{1152} \right) \\ \tau L/M &= \frac{\pi^2 \tilde{\epsilon}}{6} - \frac{\pi^4 \tilde{\epsilon}^2}{36} , \end{aligned} \quad (4.20)$$

where the small parameter is defined through  $\tilde{\epsilon} = \mu_M^2/L^2 = 8G_5 M/(3\pi L^2)$ .

The first order thermodynamics results are available for arbitrary  $D$  [17, 16], and were mostly confirmed numerically [20, 21]

$$S = \frac{\Omega_{D-3}}{4} \rho_0^{D-2} \left[ 1 + \frac{D-2}{D-3} \delta \right]$$

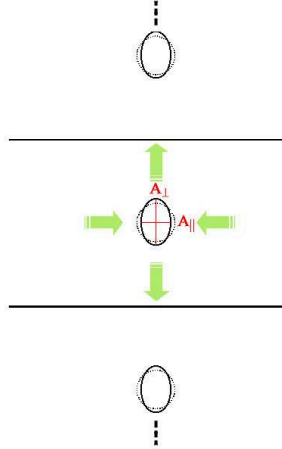


**Figure 27:** The first non-spherical deformation of the horizon is a quadrupole moment, making the black hole prolate, namely elongated along the  $z$  axis. In order to measure the eccentricity we define  $A_{\parallel}$  the area of the equator sphere and  $A_{\perp}$  the area of a “polar” sphere.

$$\begin{aligned} T &= \frac{D-3}{4\pi\rho_0} [1 - (D-2)\delta] \\ \tau L/M &= \frac{D-3}{2} \delta \\ M &= \frac{(D-2)\Omega_{D-2}}{16\pi G_N} \rho_0^{D-3} \left[ 1 + \frac{1}{2} \delta \right], \end{aligned} \quad (4.21)$$

where

$$\delta := \zeta(D-3) \left( \frac{\rho_0}{L} \right)^{D-3} \quad (4.22)$$

Some nice geometric quantities can be measured as well. The leading deviation from spherical shape is such that the BH becomes elongated along the  $z$  axis, namely prolate – see figure 27. Its eccentricity can be measured by

$$\epsilon := \frac{A_{\perp}}{A_{\parallel}} - 1 = \frac{(D-3)^4 \Gamma^2(2 + \frac{2}{D-3}) \zeta(D-1)}{8(D-2) \Gamma(\frac{4}{D-3})} \left( \frac{\rho_0}{L} \right)^{D-1}. \quad (4.23)$$

This result actually comes from beyond first order. The inter-polar distance (going around the compact dimension, see figure 28) is given by

$$\begin{aligned} L_{\text{poles}} &= L - 2^{\frac{D-5}{D-3}} \rho_0 I_D \\ I_D &= 4^{\frac{1}{D-3}} \sqrt{\pi} \frac{\Gamma(\frac{D-4}{D-3})}{\Gamma(\frac{1}{2} - \frac{1}{D-3})}. \end{aligned} \quad (4.24)$$

Since  $I_5 = 0$  in 5d the black hole makes room for itself, exactly compensating its size, and for that reason it was called “*the black hole Archimedes effect*”. For higher  $D$ ,  $0 < I_D < 1$  and the effect is milder.

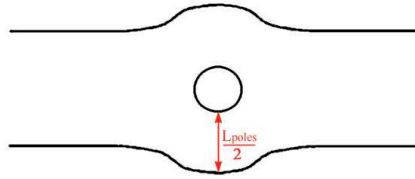


**Figure 28:** The inter-polar distance is defined to be the proper distance between the poles, going around the compact dimension. The figure depicts the tendency of mass to “make room for itself” or “the black hole Archimedes effect”.

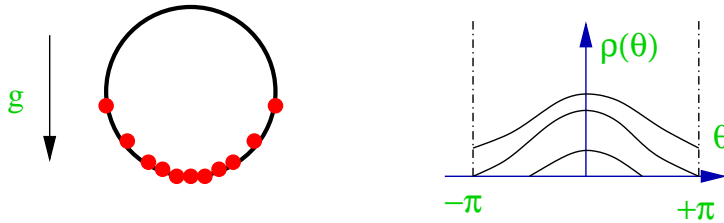


**Figure 29:** In the Gross-Witten phase transition [54] the dynamics of the eigenvalues of a unitary matrix in gauge theory is mapped to a system of particles in a horizontal loop in the field of gravity. In large  $N$  (the number of particles) the particle density becomes a continuous function  $\rho(\theta)$ . The phase transition is between localized to non-uniform and then to uniform distributions. Susskind (1997) identified this phenomenon as the gauge theory dual of the black-hole black-string transition.

## 5. Related work

Here we mention some related work.

**Relation with gauge theory & charged black holes.** The gravitational phase transition is closely related to a gauge theory phase transition, the so-called “Gross-Witten” transition [54] where the eigenvalues of some unitary matrix (originally a Wilson line over a plaquette, in a later application [55], a Wilson line around a compact dimension) change from a clumped distribution to a uniform one as the temperature is raised (see figure 29). This correspondence was first noted by Susskind (1997) [56] on a somewhat qualitative level and more recently was fully analyzed quantitatively by Aharony-Marsano-Minwalla-Wiseman in [55]. The correspondence with gauge theory enriches the system by adding another parameter to the problem – the coupling.

In [57] the authors showed that the phase diagram of black holes/strings directly maps onto the phase diagram of near-extremal black branes, and hence via holography onto the

phase diagram of the dual non-gravitational theories (Super-Yang-Mills and “Little String Theory”). More specifically, they present the phases of the non-gravitational theories and analytical results for the thermodynamics of the localized phase and the new non-uniform phase (connected to the “image” of the GL point). In fact part of the early motivation of these authors for studying black holes in Kaluza-Klein backgrounds (see [45]) has been precisely that, namely to relate it to gauge theories.

In [58] the GL analysis was generalized to charged strings, and the instability was found to persist for all charges, and moreover  $k_{GL}$  diverges as extremality is approached.

For ideas about the relation of this phase transition to the Hagedorn phase transition in string theory see [59] and references therein.

**Bubbles.** Taking the metric of the black string (2.3) and performing a double analytic continuation in  $z, t$  (namely  $t' = iz$ ,  $z' = it$ ) one gets an unstable metric called the “bubble”. In the Euclidean setting the analog would be to exchange  $\beta \leftrightarrow L$  thereby inverting  $\mu_\beta$ , which is not that interesting. From the Lorentzian perspective this is another phase that could be put on the same phase diagram. It has the special property  $\tau L = (D - 3)M$ . Thus the bubble exactly saturates the Strong Energy Condition upper bound on tension (see subsection 3.1), which motivated [36] to study this phase as well as combinations of several bubbles and BHs. So far bubble phases were not seen to connect with the phases discussed in this review, so it is conceivable that the two issues are decoupled.

**Braneworld black holes.** The topic of black holes on braneworlds is closely related to the subject of this review. There the dimensionless parameter is the ratio of the black hole size and the size of AdS. A comprehensive bibliography is beyond the scope of this paper, but we shall only mention braneworld work [49, 60, 46, 61] which was followed by work on compact dimensions.

## 6. Summary and Open questions

**Why review.** The Gregory-Laflamme instability and the whole black-hole black-string transition have been attracting constant attention in the String Theory community as well as in General Relativity since its discovery (1993).<sup>15</sup> More than three years ago the interest rose further due to the provoking ideas in [28]. A year later I suggested in [29] a qualitative form for the phase diagram which proposed the merger of the black hole and black string phases, and rested on Morse theory and a topology change analysis. Even today that paper includes most of what I know about the system, but back then many felt that the evidence was not convincing enough, and the paper was even refused for publication by two leading journals. The non-trivial nature of these predictions is best illustrated by the various other possibilities that were considered in the literature, see for example the six scenarios in [44], section 6.

Now, after more than two years and more than 30 papers, we have a much more detailed knowledge of the phase diagram, culminating in the numeric results of [22] which combine

---

<sup>15</sup>with a steady flux of about 20 citations/year.

new numerical data for black holes with older data for non-uniform strings into a full phase diagram (figure 16) exhibiting the merger of the phases predicted in [29].

Below we summarize the results, including two big surprises: critical dimensions and topology change, but we remind the reader that while there was much progress in understanding the static phase diagram, there was practically no progress towards the deeper issues regarding time evolution and singularities.

## 6.1 Results

- Confirmation of emerging phase diagram.

The current understanding of the qualitative features of the phase diagram is summarized in figure 14, whose  $D \leq 13$  case originates in [29]. All diagrams include a merger point.

For  $D \leq 13$  the end-point of decay is seen to be a black hole, and not an stable black string which was predicted in [28]. The evidence for that includes a numerical determination of practically the whole branch of the non-uniform string which emerges from the GL point and was found to have higher mass than the critical string and thus cannot serve as an end-point for decay [39]; the continued collapse of a time evolution simulation [50], coming to a stop due to grid stretching, rather than the predicted stabilization; theoretical difficulties in proposing a phase diagram which includes the predicted phase and satisfy the Morse theory constraint [29]; and finally the fact that such a phase was not found neither analytically (see the attempt of [62]) nor numerically.

For  $D \geq 14$  the end-point of (smooth) decay does turn out to be a stable non-uniform string (as a result of [27]), thus partially vindicating [28]. However, I claim that in a deeper sense, this case does not validate the arguments of [28]. First, the arguments were independent of dimension, and second, even for  $D \geq 14$ , horizon pinching, which [28] finds to be forbidden, must happen after the non-uniform string evaporates enough.

Thus while the claim of [28] stimulated much of the research reported here, and while there is no doubt regarding the calculations presented there, we find strong (actually, overwhelming in my opinion) evidence against it. That means that if something went wrong in the arguments of [28] it is rather deep and there are lessons to be learned from it. Indeed there is a clear suspect for that – the reliance on the increasing area of the event horizon. Even though the authors were careful to use a version of the theorem valid even if there is a singularity on the horizon, I suspect that either the notion of the event horizon is ill-defined here and/or that the singularity completely leaves the horizon. The problem with the definition of the event horizon is that if a singular shock wave emerges from a naked singularity and reaches null infinity, then we do not have the asymptotically Minkowski null infinity which is normally used in the definition. Clearly, this problem is not fully understood, much like other issues regarding the time evolution.

- Critical dimensions.

The stability of cones, which have a role in the local model for merger, exhibits a critical dimension  $D_{\text{merger}}^* = 10$  [29]. At a different point in the phase diagram, the GL instability changes from explosive (first order) to smooth (second order) for  $D > D_{GL}^* = 13.5$ , as was shown by Sorkin [27]. There are indications that by using a higher dimensional torus rather than  $\mathbf{S}^1$   $D_{GL}^*$  may be lowered [11] but the computation was not completed yet.

These critical dimensions are fascinating, but it is not known whether they have a deeper, wider meaning. The critical dimension of the BKL theory of the approach to a space-like singularity,  $D^* = 10$ , is closely related. On the one hand one cannot help wondering whether there could be a connection with the critical dimension for super-strings, 10d, but on the other hand the derivations and issues involved differ widely, for example, in the phase transition no supersymmetry is involved while it is central for the super-string.

- The “merger” topology change [29].

The spaces of metrics for two different topologies, the Euclidean black string and the black hole (in  $D \geq 5$ ) are glued together and a line of Ricci flat solutions connects them (in finite distance).

Additional results include

- Using Morse theory in GR [29].
- The role of tension and the first law for this system [31, 19].
- Formulating Gravito-statics by relaxation (in 2d) [39].
- Numerical experiments: strings [39], black holes [20, 21, 22] and a dynamic time-evolution [50].
- Developing an analytic perturbation method for small caged black holes – “a dialogue of multipoles” [17, 18]. See [16] for a different analytic method.

## 6.2 Open questions

We list some open questions.

- The deepest questions: are there a naked singularity and a singular shock wave in the time evolution? – see the discussion in subsection 2.4.
- Determine the critical dimension for torus compactifications (in progress).
- Stability analysis in the micro-canonical ensemble. In the canonical ensemble the Morse analysis, which identifies the thermodynamic potential  $F$  with a Morse function, allows us to read the stability of phases off the phase diagram. It is plausible that a generalization to other ensembles exists (in progress). For instance, that would

allow to settle the conjectured (micro-canonical) instability of the non-uniform string (for  $D < 14$ ).

- Gubser and Mitra [63] conjectured already in 2000 a connection between perturbative and thermodynamic instabilities of strings which is closely related to the issues of this review. It would be interesting to settle this conjecture.
- Formulate gravito-statics in more than 2d.
- Numerically trace the phase diagram also for additional dimensions in the ranges  $10 < D \leq 13$  and  $D \geq 14$ .
- Run a time evolution for  $D \geq 14$  to observe the second order transition.

**The ring.** We list some questions regarding the physics of the sister system of rotating rings, even though they are not part of the main subject of this review.

- Obtain the full phase diagram: stability of phases, order of transition, critical points.
- Solutions in  $D > 5$ ?

### Acknowledgements

It is a pleasure to thank Toby Wiseman and Niels Obers for reading the paper and making comments on it, the authors of [22, 27, 50, 11, 17] for permission to reproduce their figures and especially for adapting them, in some cases, for this review; my collaborators Dan Gorbonos, Tsvi Piran, Evgeny Sorkin and Toby Wiseman with whom I worked on this topic; Hideaki Kudoh, Luis Lehner and Niels Obers for discussions and correspondence; John Bahcall, Gary Gibbons, Gary Horowitz, and Lenny Susskind for discussions and inspiration; Roberto Emparan, Steve Gubser, Akihiro Ishibashi, Igor Klebanov, Hermann Nicolai, Mukund Rangamani, Edward Witten for some specific discussions; and finally Shmu’el Elitzur, Amit Giveon, and Eliezer Rabinovici my group partners in Jerusalem for their assistance during these two first years of mine here. I also wish to thank the following institutions for their hospitality during the course of the work reviewed here: Max-Planck Institute at Golm, Humboldt University Berlin, Cambridge University, Amsterdam University, the Perimeter Institute, MIT and Harvard University.

BK is supported in part by The Israel Science Foundation (grant no 228/02) and by the Binational Science Foundation BSF-2002160.

## A. Formulae for action manipulation

Here we collect some formulae useful for manipulation of actions.

The Ricci scalar in the presence of a general fibration

$$ds^2 = ds_X^2 + \sum_i e^{2F_i} ds_{Yi}^2 \Rightarrow$$

$$R = R_X + \sum_i [e^{-2F_i} R_{Yi} - 2d_i \tilde{\Delta}(F_i) - d_i(\partial F_i)^2] - \sum_{i,j} d_i d_j (\partial F_i \cdot \partial F_j) \quad (\text{A.1})$$

where the fibration fields depend only on the  $x$  coordinates,  $R_X$ ,  $R_{Yi}$  are the Ricci scalars of the spaces  $X$ ,  $Y_i$ ,  $d_i$  are the dimensions  $\dim(Y_i)$ ,  $F_i = F_i(x)$ , and the Laplacian ( $\tilde{\Delta}$ ) and grad-squared ( $\partial \cdot \partial$ ) are evaluated in the  $X$  space.

The Ricci scalar of a conformally transformed metric (see for example [64])

$$\tilde{ds}^2 = e^{2w} ds^2 \Rightarrow$$

$$\tilde{R} = e^{-2w} [R - 2(\hat{d} - 1) \Delta w - (\hat{d} - 1)(\hat{d} - 2)(\partial w)^2] \quad (\text{A.2})$$

where  $\hat{d}$  is the dimension of the space and the Laplacian and grad-squared are evaluated in the non-tilded metric.

## B. Topology change is a finite distance away

Scaling down a smoothed cone gives a family of metrics which approaches the singular cone, as discussed in subsection 3.4 (see figure 13). In this appendix we wish to show that the singular cone is at a finite distance in moduli space, just like the conifold.

Let us denote a smooth cone metric with some specific length scale (of the smoothed tip) by

$$\tilde{ds}^2 = d\tilde{\rho}^2 + e^{2a(\tilde{\rho})} d\Omega_{\mathbf{S}^m}^2 + e^{2b(\tilde{\rho})} d\Omega_{\mathbf{S}^n}^2. \quad (\text{B.1})$$

The family of rescaled cone metrics is defined by

$$ds^2 = e^{-2\sigma} \tilde{ds}^2, \quad (\text{B.2})$$

and we wish to compute the distance in moduli space from  $\sigma = 0$  to  $\sigma = \infty$ .

The metric on moduli space can be found by adding an auxiliary coordinate  $t$ , making  $\sigma$   $t$ -dependent and evaluating its kinetic term. Since one wants to hold the asymptotic form of the cone fixed it is useful to introduce  $\rho = e^{-\sigma} \tilde{\rho}$ . Then the rescaled cone metric is  $ds^2 = d\rho^2 + e^{2(a(\rho e^\sigma) - \sigma)} d\Omega_m^2 + e^{2(b(\rho e^\sigma) - \sigma)} d\Omega_n^2$ , where  $d\Omega_m = d\Omega_{\mathbf{S}^m}^2$ . Adding  $t$ -dependence and substituting back to  $\tilde{\rho}$  we get

$$dt^2 + e^{-2\sigma} \left[ (d\tilde{\rho} - \dot{\sigma} \tilde{\rho} dt)^2 + e^{2a} d\Omega_m^2 + e^{2b} d\Omega_n^2 \right] \quad (\text{B.3})$$

Using (A.1) the Ricci scalar is

$$R = -m(m+1)(\partial(a - \sigma))^2 - 2m\Delta(a - \sigma)$$

$$-n(n+1)(\partial(b - \sigma))^2 - 2n\Delta(b - \sigma)$$

$$-2mn\partial(a - \sigma)\partial(b - \sigma), \quad (\text{B.4})$$

where the differential operators are in the  $(\tilde{\rho}, t)$  plane. All terms which are independent of  $\sigma$  must cancel since the resolved cone is Ricci-flat, and one finds

$$R = -2 \left[ (m a' + n b') \tilde{\rho} - (D - 1) \right] \ddot{\sigma} + \dot{\sigma}^2 \left[ -\tilde{\rho}^2 (m(m-1) e^{-2a} + n(n-1) e^{-2b}) + 2\tilde{\rho}(D-1)(m a' + n b') - D(D-1) \right] \quad (\text{B.5})$$

A useful test for this expression is that it must vanish when substituting the singular cone metric rather than the resolved cone.

The resulting bulk action after multiplying by  $\sqrt{g} = e^{m a + n b - D \sigma}$  and eliminating the second derivatives using integration by parts is

$$S = \int dt \dot{\sigma}^2 e^{-D\sigma} \int d\tilde{\rho} e^{m a + n b} \cdot \left[ -\tilde{\rho}^2 (m(m-1) e^{-2a} + n(n-1) e^{-2b}) - 2\tilde{\rho}(m a' + n b') + D(D-1) \right] \quad (\text{B.6})$$

This action should be regularized by comparison with the singular cone. This can be done by introducing a large-distance cut-off  $\rho = R$  and therefore  $\tilde{\rho}_R = R e^\sigma$  and subtracting for the cone. We are interested in large  $\sigma$  and hence  $\tilde{\rho}_R \rightarrow \infty$ . Therefore we are interested in the large  $\tilde{\rho}$  behavior of  $a, b$  compared to the singular cone which is given by the linearized perturbations (3.24)

$$\delta a, \delta b \sim \rho^s, \quad \text{Re}(s) = -(D-2)/2 \quad (\text{B.7})$$

The large  $\tilde{\rho}_R$  behavior of the kinetic term in (B.6) is

$$e^{-D\sigma} \int^{R e^\sigma} d\tilde{\rho} \tilde{\rho}^{D-1} \tilde{\rho}^{-(D-2)} \sim e^{-D\sigma} (R^2 e^{2\sigma}) \quad (\text{B.8})$$

Hence the metric on moduli space in the large  $\sigma$  limit is

$$ds_{\mathcal{M}}^2 = e^{-(D-2)\sigma} d\sigma^2 \quad (\text{B.9})$$

and the distance is finite

$$\int^{+\infty} \exp\left(-\frac{D-2}{2}\sigma\right) d\sigma < \infty \quad (\text{B.10})$$

for  $D > 2$ , namely always, since we were only interested in  $D \geq 5$ .

## References

- [1] R. Emparan, *Rotating circular strings, and infinite non-uniqueness of black rings*, *JHEP* **03** (2004) 064, [[hep-th/0402149](#)].
- [2] I. Bena and N. P. Warner, *One ring to rule them all ... and in the darkness bind them?*, [hep-th/0408106](#).
- [3] H. Elvang, R. Emparan, D. Mateos, and H. S. Reall, *Supersymmetric black rings and three-charge supertubes*, [hep-th/0408120](#).
- [4] B. Kol, *Speculative generalization of black hole uniqueness to higher dimensions*, [hep-th/0208056](#).
- [5] T. Damour, M. Henneaux, and H. Nicolai, *Cosmological billiards*, *Class. Quant. Grav.* **20** (2003) R145–R200, [[hep-th/0212256](#)].
- [6] R. C. Myers and M. J. Perry, *Black holes in higher dimensional space-times*, *Ann. Phys.* **172** (1986) 304.
- [7] R. Emparan and H. S. Reall, *A rotating black ring in five dimensions*, *Phys. Rev. Lett.* **88** (2002) 101101, [[hep-th/0110260](#)].
- [8] H. Elvang, R. Emparan, D. Mateos, and H. S. Reall, *A supersymmetric black ring*, [hep-th/0407065](#).
- [9] J. P. Gauntlett and J. B. Gutowski, *Concentric black rings*, [hep-th/0408010](#).
- [10] J. P. Gauntlett and J. B. Gutowski, *General concentric black rings*, [hep-th/0408122](#).
- [11] B. Kol and E. Sorkin, *On black-brane instability in an arbitrary dimension*, [gr-qc/0407058](#).
- [12] R. C. Myers, *Higher dimensional black holes in compactified space-times*, *Phys. Rev.* **D35** (1987) 455.
- [13] D. Korotkin and H. Nicolai, *A periodic analog of the Schwarzschild solution*, [gr-qc/9403029](#).
- [14] A. V. Frolov and V. P. Frolov, *Black holes in a compactified spacetime*, *Phys. Rev.* **D67** (2003) 124025, [[hep-th/0302085](#)].
- [15] F. R. Tangherlini, *Schwarzschild field in  $n$  dimensions and the dimensionality of space problem*, *Nuovo Cim.* **27** (1963) 636.
- [16] T. Harmark, *Small black holes on cylinders*, *Phys. Rev.* **D69** (2004) 104015, [[hep-th/0310259](#)].
- [17] D. Gorbonos and B. Kol, *A dialogue of multipoles: Matched asymptotic expansion for caged black holes*, *JHEP* **06** (2004) 053, [[hep-th/0406002](#)].
- [18] D. Karasik, C. Sahabandu, P. Suranyi, and L. C. R. Wijewardhana, *Analytic approximation to 5 dimensional black holes with one compact dimension*, [hep-th/0410078](#).
- [19] B. Kol, E. Sorkin, and T. Piran, *Caged black holes: Black holes in compactified spacetimes. I: Theory*, *Phys. Rev.* **D69** (2004) 064031, [[hep-th/0309190](#)].
- [20] E. Sorkin, B. Kol, and T. Piran, *Caged black holes: Black holes in compactified spacetimes. II: 5d numerical implementation*, *Phys. Rev.* **D69** (2004) 064032, [[hep-th/0310096](#)].
- [21] H. Kudoh and T. Wiseman, *Properties of Kaluza-Klein black holes*, *Prog. Theor. Phys.* **111** (2004) 475–507, [[hep-th/0310104](#)].

- [22] H. Kudoh and T. Wiseman, *Connecting black holes and black strings*, [hep-th/0409111](#).
- [23] R. Gregory and R. Laflamme, *Black strings and p-branes are unstable*, *Phys. Rev. Lett.* **70** (1993) 2837–2840, [[hep-th/9301052](#)].
- [24] R. Gregory and R. Laflamme, *Hypercylindrical black holes*, *Phys. Rev.* **D37** (1988) 305.
- [25] R. Gregory and R. Laflamme, *The instability of charged black strings and p-branes*, *Nucl. Phys.* **B428** (1994) 399–434, [[hep-th/9404071](#)].
- [26] D. J. Gross, M. J. Perry, and L. G. Yaffe, *Instability of flat space at finite temperature*, *Phys. Rev.* **D25** (1982) 330–355.
- [27] E. Sorkin, *A critical dimension in the black-string phase transition*, *Phys. Rev. Lett.* **93** (2004) 031601, [[hep-th/0402216](#)].
- [28] G. T. Horowitz and K. Maeda, *Fate of the black string instability*, *Phys. Rev. Lett.* **87** (2001) 131301, [[hep-th/0105111](#)].
- [29] B. Kol, *Topology change in general relativity and the black-hole black-string transition*, [hep-th/0206220](#).
- [30] B. Kol, *Explosive black hole fission and fusion in large extra dimensions*, [hep-ph/0207037](#).
- [31] T. Harmark and N. A. Obers, *New phase diagram for black holes and strings on cylinders*, *Class. Quant. Grav.* **21** (2004) 1709, [[hep-th/0309116](#)].
- [32] J. H. Traschen and D. Fox, *Tension perturbations of black brane spacetimes*, *Class. Quant. Grav.* **21** (2004) 289–306, [[gr-qc/0103106](#)].
- [33] P. K. Townsend and M. Zamaklar, *The first law of black brane mechanics*, *Class. Quant. Grav.* **18** (2001) 5269–5286, [[hep-th/0107228](#)].
- [34] J. H. Traschen, *A positivity theorem for gravitational tension in brane spacetimes*, *Class. Quant. Grav.* **21** (2004) 1343–1350, [[hep-th/0308173](#)].
- [35] T. Shiromizu, D. Ida, and S. Tomizawa, *Kinematical bound in asymptotically translationally invariant spacetimes*, *Phys. Rev.* **D69** (2004) 027503, [[gr-qc/0309061](#)].
- [36] H. Elvang, T. Harmark, and N. A. Obers, *Sequences of bubbles and holes: New phases of Kaluza-Klein black holes*, [hep-th/0407050](#).
- [37] T. Harmark and N. A. Obers, *General definition of gravitational tension*, *JHEP* **05** (2004) 043, [[hep-th/0403103](#)].
- [38] S. S. Gubser, *On non-uniform black branes*, *Class. Quant. Grav.* **19** (2002) 4825–4844, [[hep-th/0110193](#)].
- [39] T. Wiseman, *Static axisymmetric vacuum solutions and non-uniform black strings*, *Class. Quant. Grav.* **20** (2003) 1137–1176, [[hep-th/0209051](#)].
- [40] M.-I. Park, *The final state of black strings and p-branes, and the Gregory-Laflamme instability*, [hep-th/0405045](#).
- [41] B. Kol and T. Wiseman, *Evidence that highly non-uniform black strings have a conical waist*, *Class. Quant. Grav.* **20** (2003) 3493–3504, [[hep-th/0304070](#)].
- [42] I. Klebanov, M. Rangamani, and E. Witten. private communication.
- [43] L. D. Landau and E. M. Lifshitz, *Quantum mechanics*. Pergamon, 1977. §35.

- [44] T. Harmark and N. A. Obers, *Phase structure of black holes and strings on cylinders*, *Nucl. Phys.* **B684** (2004) 183–208, [[hep-th/0309230](#)].
- [45] T. Harmark and N. A. Obers, *Black holes on cylinders*, *JHEP* **05** (2002) 032, [[hep-th/0204047](#)].
- [46] H. Kudoh, T. Tanaka, and T. Nakamura, *Small localized black holes in braneworld: Formulation and numerical method*, *Phys. Rev.* **D68** (2003) 024035, [[gr-qc/0301089](#)].
- [47] T. Wiseman, *From black strings to black holes*, *Class. Quant. Grav.* **20** (2003) 1177–1186, [[hep-th/0211028](#)].
- [48] B. Kol and M. Rodriguez-Martinez. unpublished.
- [49] T. Wiseman, *Relativistic stars in Randall-Sundrum gravity*, *Phys. Rev.* **D65** (2002) 124007, [[hep-th/0111057](#)].
- [50] M. W. Choptuik *et. al.*, *Towards the final fate of an unstable black string*, *Phys. Rev.* **D68** (2003) 044001, [[gr-qc/0304085](#)].
- [51] T. Regge and J. A. Wheeler, *Stability of a Schwarzschild singularity*, *Phys. Rev.* **108** (1957) 1063–1069.
- [52] H. Kodama and A. Ishibashi, *A master equation for gravitational perturbations of maximally symmetric black holes in higher dimensions*, *Prog. Theor. Phys.* **110** (2003) 701–722, [[hep-th/0305147](#)].
- [53] D. Gorbonos and B. Kol. to appear.
- [54] D. J. Gross and E. Witten, *Possible third order phase transition in the large  $N$  lattice gauge theory*, *Phys. Rev.* **D21** (1980) 446–453.
- [55] O. Aharony, J. Marsano, S. Minwalla, and T. Wiseman, *Black hole - black string phase transitions in thermal 1+1 dimensional supersymmetric Yang-Mills theory on a circle*, [hep-th/0406210](#).
- [56] L. Susskind, *Matrix theory black holes and the Gross Witten transition*, [hep-th/9805115](#).
- [57] T. Harmark and N. A. Obers, *New phases of near-extremal branes on a circle*, [hep-th/0407094](#).
- [58] O. Sarbach and L. Lehner, *Critical bubbles and implications for critical black strings*, [hep-th/0407265](#).
- [59] J. L. F. Barbon and E. Rabinovici, *Touring the Hagedorn ridge*, [hep-th/0407236](#).
- [60] D. Karasik, C. Sahabandu, P. Suranyi, and L. C. R. Wijewardhana, *Small (1-TeV) black holes in Randall-Sundrum I scenario*, *Phys. Rev.* **D69** (2004) 064022, [[gr-qc/0309076](#)].
- [61] H. Kudoh, *Thermodynamical properties of small localized black hole*, *Prog. Theor. Phys.* **110** (2004) 1059–1069, [[hep-th/0306067](#)].
- [62] P.-J. De Smet, *Black holes on cylinders are not algebraically special*, *Class. Quant. Grav.* **19** (2002) 4877–4896, [[hep-th/0206106](#)].
- [63] S. S. Gubser and I. Mitra, *Instability of charged black holes in anti-de Sitter space*, [hep-th/0009126](#).
- [64] R. M. Wald, *General Relativity*. The University of Chicago Press, 1984. appendix D.